Miner Petrol (2008) 94:287–303
DOI 10.1007/s00710-008-0018-1

ORIGINAL PAPER

# Evolution of volcanism in graben and horst structures along the Cenozoic Cameroon Line (Africa): implications for tectonic evolution and mantle source composition

**D. G. Nkouathio · A. Kagou Dongmo · J. M. Bardintzeff · P. Wandji · H. Bellon · A. Pouclet**

Received: 7 July 2007 / Accepted: 15 July 2008 / Published online: 18 September 2008


**Abstract** Tombel graben and Mounts Bambouto are two volcanic fields of the typical system of alternating graben and horst structure of the Cameroon Volcanic Line. Tombel graben is a young volcanic field, whereas Mounts Bambouto horst is an old stratovolcano with calderas. Volcanic products in both settings have a signature close to that of Ocean Island Basalt implying a major role of FOZO (focal zone) component and varied contribution of depleted mantle (DMM) and enriched mantle (EM) components. The Cameroon Volcanic Line is a hot line essentially resulting from passive rifting. Eocene to Recent intraplate basaltic volcanism in the study area was probably a result of mantle upwelling coupled with lithospheric extension. The olivine basaltic magma of horst volcanoes evolved in a large-scale, steady-state magmatic reservoir via crystal fractionation and limited contamination to highly differentiated alkaline lavas (trachyte and phonolite). Conversely, rapid ascent of lavas along multiple fault lines of graben structures produced less evolved lavas (hawaiite) within small reservoirs. This model, evaluated for the study area, involves mantle upwelling inside zones of weakness in the lithosphere after intra-continental extension. It can be applied to other parts of the Cameroon Volcanic Line as well, and is similar to that described in other intra-continental rift-related areas in Africa.

Editorial handling: M. Okrusch

D. G. Nkouathio · A. Kagou Dongmo
Département des Sciences de la Terre, Faculté des Sciences,
Université de Dschang,
Dschang, Cameroon

J. M. Bardintzeff (✉)
Laboratoire de Pétrographie-Volcanologie,
Université de Paris-Sud,
Bât. 504,
91405 Orsay Cédex, France
e-mail: jacques-marie.bardintzeff@u-psud.fr

J. M. Bardintzeff
IUFM, Université de Cergy-Pontoise,
Versailles, France

P. Wandji
Laboratoire de géologie, Ecole Normale Supérieure,
Université de Yaoundé I,
Yaoundé, Cameroon

H. Bellon
UMR 6538 Domaines océaniques, IUEM,
Université de Bretagne Occidentale,
Brest, France

A. Pouclet
Olivet, France

## Introduction

The Cameroon Volcanic Line (CVL) is a prominent, 1,600 km long within-plate geological feature in central Africa (Fig. 1a). This structure is characterized by an alternation of horsts and grabens. Various types of volcanic structures are present within this alignment. The CVL extends over both the Atlantic oceanic lithosphere (post-Jurassic, 120 Ma), and the Pan-African continental lithosphere (600 Ma). Between these, there is a transitional domain, defined seismically as “Continental Ocean Boundary” (Halliday et al. 1988; Lee et al. 1994).

In this paper, we summarize the main characteristics of associated Neogene to Quaternary volcanism in the continental southern part of the CVL. We attempt to describe the evolution of volcanism along the Cameroon Line using a comparison between a typical graben volcano (Tombel graben)

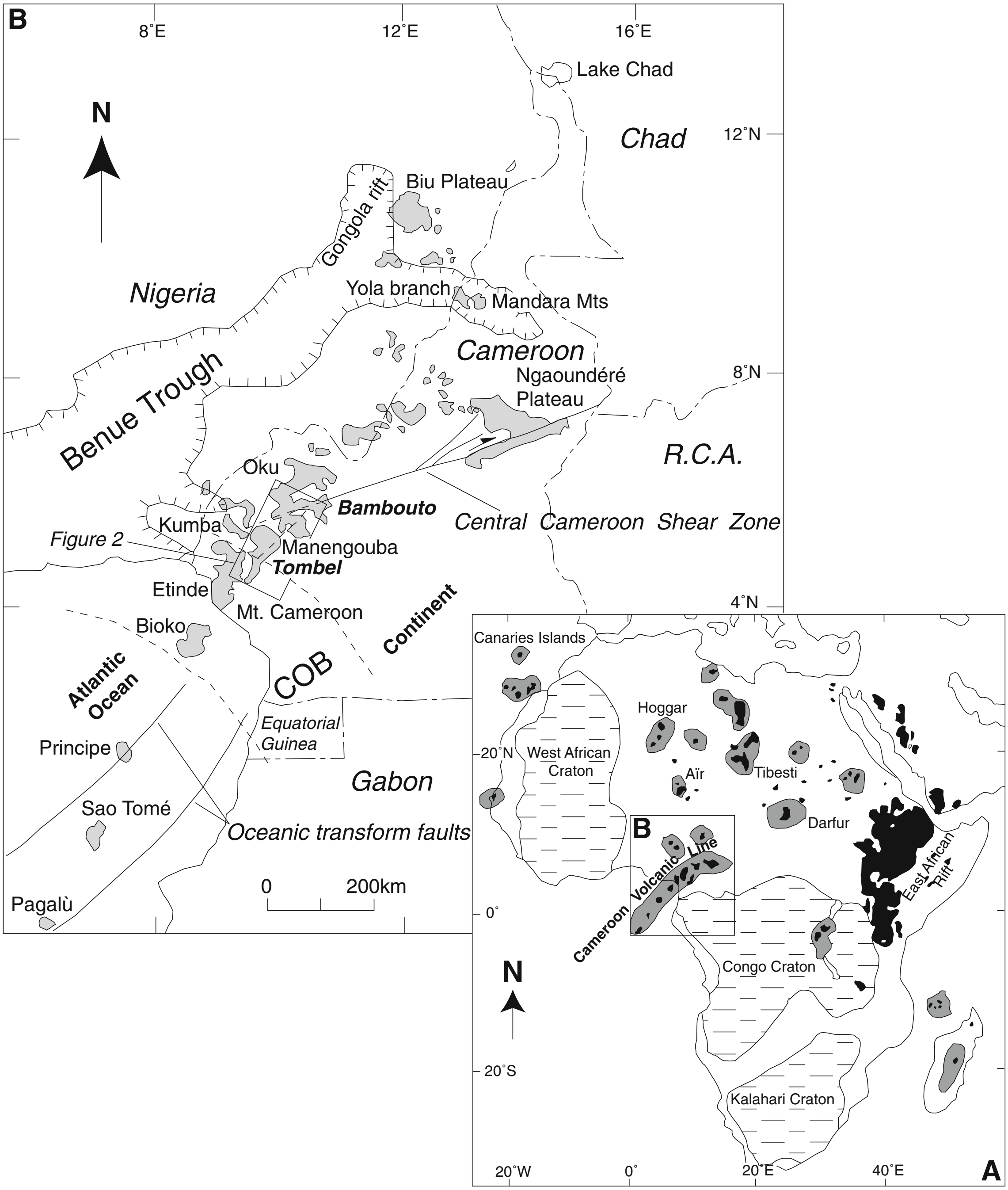


**Fig. 1** **A** Location map of the Cameroon Volcanic Line (CVL). The main geologic features of Africa are indicated. **B** The main volcanic centres of the Cameroon Volcanic Line. COB Continental Ocean Boundary. *Dashed lines* are limits between the CVL segments: ocean, COB and continent. Central Cameroon Shear Zone according to Ngako et al. (2006); Fracture zones following Lee et al. (1994) and Ballentine et al. (1997). The *rectangle* marks the study area (Fig. 2)

and a horst volcano (Mounts Bambouto and surrounding flood basalt of Western Highlands) of the CVL. These regions provide an excellent example of continental within-plate volcanism in a peculiar tectonic environment. We present new mineralogical, geochronological, geochemical and isotopic (Sr, Nd) data on lavas from the Tombel graben and the Mounts Bambouto volcanoes. The final aim of this study is to examine whether these new data comply with one of the various hypotheses available about the origin of the CVL. Since this is a subject of controversy, we will discuss the tectonic and geochemical data bearing on the two main propositions:

- A stagnant hot line or a fissure tapping a hot asthenopheric zone (Meyers et al. 1998; Montigny et al. 2004; Pik et al. 2006).
- An active rift system produced by a thermal anomaly in the asthenosphere which could be responsible for the Y-shaped form of the CVL that resembles the Benue trough (Fig. 1b) (Fitton 1983, 1987; Déruelle et al. 1991; Wilson and Guiraud 1992; Maluski et al. 1995).

Our propositions, presented here, are based on different petrogenetic models for the origin of lavas in each of these environments.

## Geological background

### Geotectonic context

The CVL is interpreted as a megashear zone that seems to be structurally subdivided by an important network of faults associated with a system of alternating horsts and grabens (Gèze 1943; Déruelle et al. 1991). This structure is characterized by a SW–NE alignment (trending 30°) of both oceanic and continental volcanic massifs and plutons extending from Pagalù Island to Lake Chad (Fig. 1b). The oceanic part lies within the gulf of Guinea and comprises the islands of Pagalù, Sao Tomé, Principe and Bioko. The continental domain is characterised by (1) large strato-volcanoes and central type volcanic massifs, occasionally with calderas (Mounts Cameroon, Manengouba, Bambouto, Bamenda, Oku), (2) collapsed plains which are filled with sediments and occupied by monogenetic volcanoes (Tombel, Noun, Kumba, Ngaoundéré) as well as flood basalts, (3) volcanic necks and plugs (Kapsiki, Mandara).

The Tombel graben is an Upper Miocene warped trough (Kueté and Dikoumé 2000) recently filled up by lava flows, juxtaposed to the Manengouba stratovolcano. The Tombel graben volcanic field is very close to the Continental Ocean Boundary of the CVL (Fig. 1b). It is located at 4°32′–4°58°N and 9°35′–9°51′E (Fig. 2) and covers a surface area of about 800 $km^2$. The Tombel graben represents one of the highest concentration of monogenetic volcanoes along the CVL, and includes more than 100 Quaternary scoria cones with associated lava flows. Two main eruptive styles occurred in this region: the effusive style of the Lower Volcanic Unit (LVU) was followed by a more explosive style of the Upper Volcanic Unit (UVU; Nkouathio et al. 2002; Nkouathio 2006).

The Mounts Bambouto horst, like Mounts Cameroon, Manengouba, Bamenda, Oku, is a large composite volcano standing on the thick flood basalts of the Western Highlands. The Mounts Bambouto exhibit the main characteristics of all these central volcanoes. It is a shield volcano, that lies between 10°–10°10′E and 5°35′–5°45°N, along the SW–NE linear axis which includes Mounts Cameroon and Manengouba (Figs. 1 and 2). It is elliptical (45–50×20–25 km) and bears a collapse caldera (13×8 km) at its summit. At this volcano, an alternation of four eruption styles can be observed: lava flows, domes, strombolian eruptions, and ignimbrite-forming pyroclastic flows.

### Current petrogenetic models

The Western and Central African volcanism is characterized by either large lithospheric domes or swells such as the Hoggar, Aïr, Tibesti, Darfur, East African system and CVL (Fig. 1a) (Chorowicz 2005; Pik et al. 2006). CVL as well as many other volcanic provinces across the African plate are characterized by associations of Tertiary to recent volcanism. Geochemically, the volcanic rocks of CVL are almost identical in both oceanic and continental regions. They are dominantly alkali-rich OIB, having the same trace element abundances, rich in large-ion lithophile elements (LILE). This implies a related, upper mantle source from somewhere above the 670 km transition zone (Halliday et al. 1988, 1990; Lee et al. 1994). However, some tholeiitic and transitional affinities have been described and discussed recently (Ngounouno et al. 2001; Moundi 2004; Fosso et al. 2005; Kuepouo et al. 2006; Moundi et al. 2007). Young basaltic lavas are identical in composition in both oceanic and continental sectors, suggesting that the magmas have been derived from identical asthenospheric sources.

Ballentine et al. (1997) argued that the entire CVL appeared to have its origins in HIMU mantle, and mantle metasomatism has been invoked by Fitton and Dunlop (1985). However, higher $^{206}Pb/^{204}Pb$ ratios that have been observed, since these publications, in lavas of Continental Ocean Boundary appear to be caused by extreme U/Pb fractionation brought about during Mesozoic enrichment within the Upper Mantle (Halliday et al. 1990; Ballentine et al. 1997). Woodhead (1996) considered the signature of the basalt between HIMU and EM types to reflect simple mixing between subducted oceanic crust and sediment sources. A focal zone (FOZO) component has been recently invoked (Stracke et al. 2005; Déruelle et al. 2007). The CVL as a whole is considered to have developed along lithosphere discontinuities within the African plate. Mantle upwelling is favoured inside weakness zones of the lithosphere after intra-continental extension. These rift faults may act as channels for mantle fluids (Bailey 1987). The present debate (e.g., Pik et al. 2006) concerns the type of mantle dome (mantle hotspot or hot line) and the upwelling mechanism.

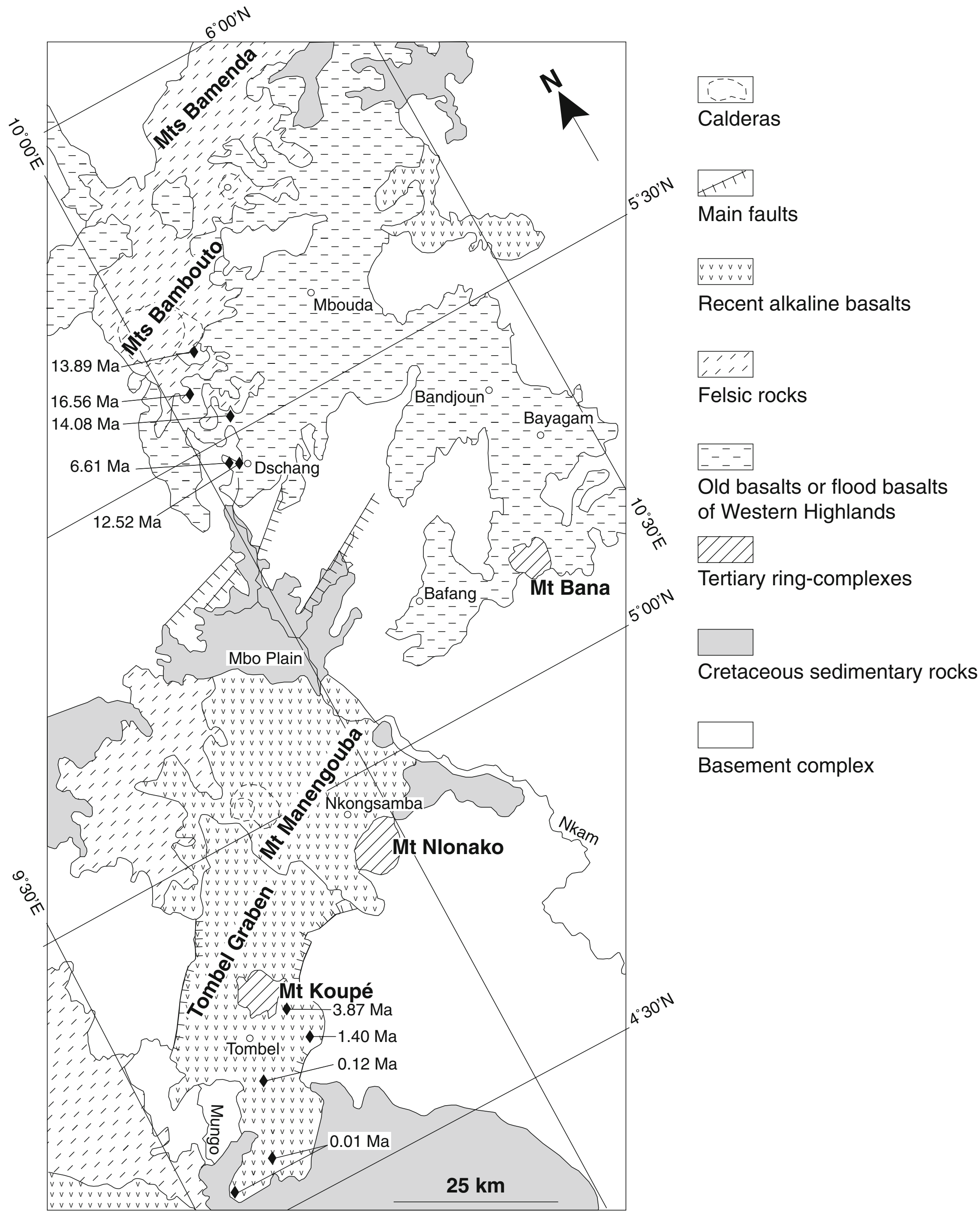


**Fig. 2** Geological sketch map of the studied continental part of the CVL, showing Tombel graben and Mounts Bambouto (after Dumort 1968, modified)

## Volcanostratigraphy and new geochronological data

### Analytical methods

Ten new age determinations have been obtained for different lava types from volcanic rocks of Tombel graben and Mounts Bambouto. Sample without xenocrysts have been preferentially chosen. The $^{40}K$–$^{40}Ar$ age dating has been carried out on whole rock samples. The samples were crushed and sieved to 0.315–0.160 mm grain size, and then cleaned with distilled water. After reduction to powder, potassium analysis was done by atomic absorption spectrometry after hydrofluoric acid ($H_2F_2$) attack. The grained fraction was used for argon extraction by high frequency heating under high vacuum. Age calculations were carried out using the constants recommended by Steiger and Jäger (1977). In addition, several volcanic rocks of Mounts Bambouto have already been dated (Tchoua 1974; Fitton 1983; Youmen 1994; Marzoli et al. 1999, 2000). All these ages are reported in Fig. 3.

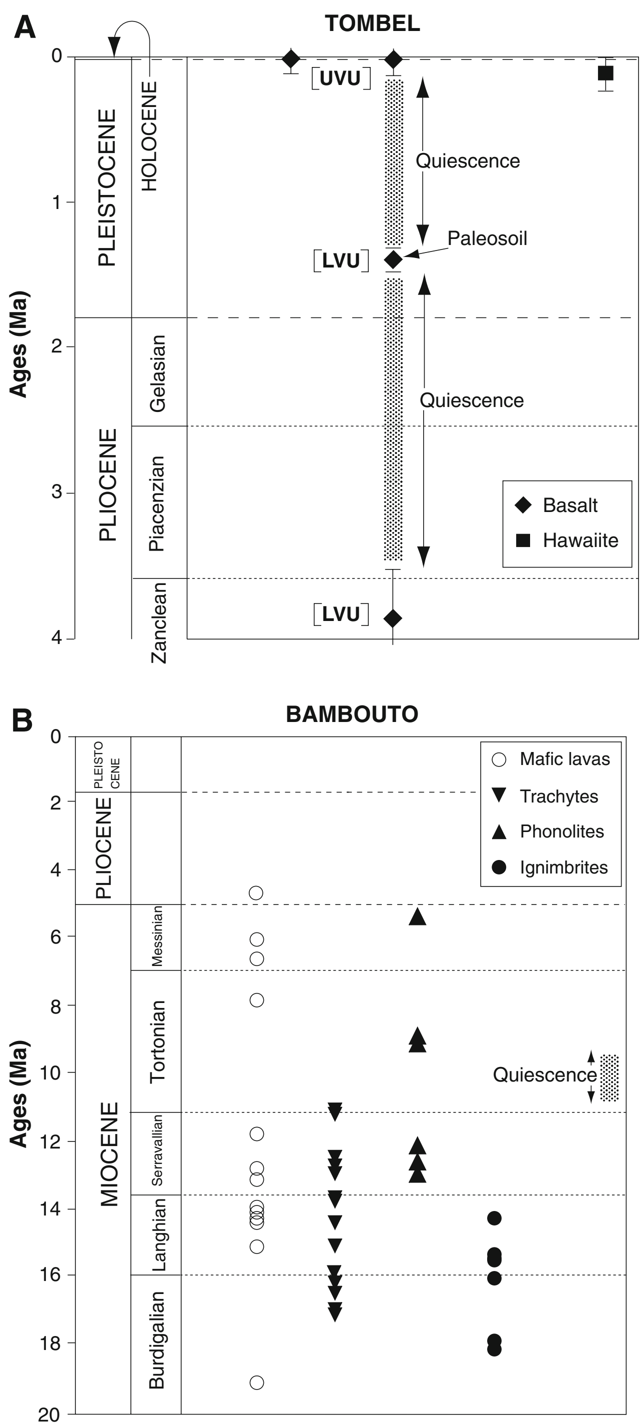


**Fig. 3** K–Ar ages of volcanic rocks of Tombel graben and Mounts Bambouto and their position on the geological time scale

## Results and interpretation

In Tombel graben, field observations in combination with five representative new K-Ar ages, determined on whole rock samples, allow us to clearly distinguish three major volcanic phases (Fig. 3a), i.e. two in the Lower Volcanic Unit (LVU) and one in the Upper Volcanic Unit (UVU). (1) The Lower Volcanic Unit (TPL1, TL5, Table 1) consists mainly of columnar basaltic flows. Judging from field observations and new age determinations, we can identify two periods of quiescence and an intermittent formation of paleosoil on the erupted basalt. (2) After these two periods of quiescence, each of which lasted about 1.5 Ma, a more strombolian activity occurred during the last 100 ky (NT15, NT30 and TL1, Table 1) and produced cinder cones and small lava flows forming the Upper Volcanic Unit. We notice that similar young ages have been found in the Manengouba volcano (Kagou Dongmo et al. 2001; Kagou Dongmo 2006), implying simultaneous activity and a possible common origin for lavas of both volcanoes.

The Mounts Bambouto composite volcano was emplaced on the old flood basalts of the Western Highlands, whereas a part of volcanic rocks of the Tombel graben rests unconformably on these basalts at the southern end of the structure. Age determinations of these old flood basalts range from 51.8 to 44.0 Ma (Tchoua 1974; Fosso et al. 2005; Moundi et al. 2007). Lithic fragments in the ignimbrites of the Mounts Bambouto described by Nono et al. (2004) could be remnants of the old basaltic phase or of the initial activity of Mounts Bambouto.

Three main periods of volcanic activity have been recognized on Mounts Bambouto on the basis of these new data and field observations:

- *Pre-caldera magmatism*: the volcanic history of Mounts Bambouto started in the Burdigalian as indicated by a Ar–Ar date of 19 Ma (Marzoli et al. 1999). The eruption of fissure-related basalt was associated with strombolian activity. The remnants of these rocks (scoriae) are seen in non-welded tuffs and ignimbrites on the southern flank of the mountain (Nono et al. 2004).
- *Caldera forming eruption*: this was the main volcanic episode during which a large volume of magma escaped explosively (as ignimbrites), from a shallow reservoir, permitting roof collapse. This produced thick pyroclastic rocks (trachyte and scarce rhyolite, Youmen 1994) associated with lava flows (mainly trachyte) that were deposited on the caldera rims. These lavas and tephras erupted from 18.1±0.01 Ma (Burdigalian) to 11.1±0.02 Ma (Tortonian, Fig. 3b) (Youmen 1994; Marzoli et al. 1999, 2000; Nkouathio 2006).
- *Post-caldera phase*: age determinations for post-caldera units range from 7.75±0.01 Ma to 4.52±0.28 Ma

**Table 1** Whole rock $^{40}K$–$^{40}Ar$ isotopic ages for selected lavas from Tombel and Bambouto volcanoes (Université de Brest, France, see text)

| Sample | Locality | Type | Analysis Reference | Age (Ma) ± Error at 1 σ | $^{36}Ar_{exp}$ ($10^{-9}$ $cm^3$) | $^{40}Ar^*$ (%) | $^{40}Ar^*/g$ ($10^{-7}$ $cm^3/g$) | $K_2O$ (wt%) | Weight (g) |
|---|---|---|---|---|---|---|---|---|---|
| NT15 | Njombé, Tombel | Basalt | B6655-2 | 0.01±0.12 | 2.01 | 0.1 | 0.004 | 1.47 | 1.0043 |
| NT30 | Njombé, Tombel | Basalt | B6656-3 | 0.01±0.11 | 1.24 | 0.0 | 0.002 | 0.99 | 1.0027 |
| TL1 | Nlohé, Tombel | Hawaiite | B6657-4 | 0.12±0.12 | 1.60 | 1.0 | 0.050 | 1.22 | 1.0059 |
| TPL1 | Loum, Tombel | Basalt | B6665-8 | 1.40±0.08 | 0.80 | 15.6 | 0.437 | 0.97 | 1.0053 |
| TL5 | Lala, Tombel | Basalt | B7014-2 | 3.87±0.62 | 2.35 | 10.8 | 1.236 | 0.99 | 0.6801 |
| NG6 | Nzindeng, Bambouto | Phonolite | B6635-4 | 6.61±0.17 | 1.31 | 49.1 | 3.735 | 1.75 | 1.0012 |
| NG1 | Nzindeng, Bambouto | Basanite | B6634-3 | 12.52±0.29 | 1.70 | 80.1 | 20.090 | 4.96 | 1.0053 |
| DB1 | Messang, Bambouto | Basanite | B6630-5 | 13.89±0.35 | 1.16 | 55.0 | 4.166 | 0.91 | 1.0100 |
| MM1 | Mebouken, Bambouto | Basanite | B6653-5 | 14.08±0.34 | 1.01 | 65.5 | 5.604 | 1.23 | 1.0063 |
| DJ1 | Djuttsita, Bambouto | Trachyte | B6636-5 | 16.72±0.39 | 1.83 | 82.9 | 26.050 | 4.81 | 1.0064 |
| | Djuttsita, Bambouto | Trachyte | B6700-3 | 16.41±0.39 | 3.12 | 73.6 | 25.560 | 4.81 | 1.0060 |

A mean age of 16.56±0.39 Ma will be considered for sample DJ1; this value is resulting from two distinct and independant experiments, from the argon extraction by fusion under vacuum to the analysis by mass spectrometry. For NT15 and NT30 samples, ages are very recent and incertitude is higher than the age.

(Youmen 1994; Marzoli et al. 1999, 2000; Nkouathio 2006). During this period, dikes, lava flows and extrusive domes cut and overlie intra- and extra-caldera volcanic rocks.

## Petrography and mineralogy

### Tombel graben

The Quaternary lavas of this region form a magmatic series from basanite to hawaiite. The lavas contain 3 to 25 vol% phenocrysts of typical alkaline assemblages made up of olivine±clinopyroxene±plagioclase±Fe–Ti oxides±amphibole. A few xenocrysts (derived from mantle xenoliths) of orthopyroxene (opx), clinopyroxene (cpx), Fe–Ti oxides and olivine have been observed in some lavas. The fine-grained groundmass consists mainly of plagioclase with olivine±clinopyroxene±Fe–Ti oxides±amphibole, with different amount of glass. Basanites contain euhedral phenocrysts of both olivine ($Fo_{87}$) and diopside up to 4 mm across and in places strongly zoned ($Wo_{43–46}En_{38–47}Fs_{13–29}$, Fig. 4a; 0–3 mol% $NaFeSi_2O_6$, 0–9 mol% $NaAlSi_2O_6$, 0–5 mol% $CaFeAlSiO_6$, 0–2 mol% $CaCrAlSiO_6$, 3–11 mol% $CaTiAl_2O_6$, 2–7 mol% $CaAl_2SiO_6$ are present). In addition, Fe–Ti oxides (mainly titanomagnetite, with variable ulvöspinel contents, and up to 16.7 mol% of spinel $MgAl_2O_4$) and plagioclase microlites are present. The investigated basalts contain phenocrysts and microphenocrysts of olivine ($Fo_{55–77}$), augite ($Wo_{34–44}En_{35–37}Fs_{10–38}$; 0–5 mol% $NaFeSi_2O_6$, 0–5 mol% $NaAlSi_2O_6$, 0–12 mol% $CaFeAlSiO_6$, 0–1 mol% $CaCrAlSiO_6$, 0–7 mol% $CaTiAl_2O_6$, 1–8 mol% $CaAl_2SiO_6$ are present), and plagioclase ($An_{79–41}$; Fig. 4b). Fe–Ti oxides of the basalts contain 95–47 mol% ulvöspinel while Fe–Ti oxides xenocrysts contain 39–35 mol% ulvöspinel. Hawaiites are characterized by abundant plagioclase ($An_{25–65}$). In some grains normal zoning is associated with augite ($Wo_{36–43}$ $En_{42–49}Fs_{20–25}$; 4–7 mol% $NaFeSi_2O_6$, 0–1 mol% $NaAlSi_2O_6$, 0–15 mol% $CaFeAlSiO_6$, 4–14 mol% $CaTiAl_2O_6$, 0–14 mol% $CaAl_2SiO_6$ are present), Ca-amphibole (pargasite, kaersutite and ferrokaersutite) and scarce olivine as microlites. Some basalts contain xenocrysts of quartz and feldspar derived from the underlying granite-gneiss basement. However, some other basalts (lava and scoria) contain mantle xenocrysts of enstatite ($Wo_{2–0}En_{83–80}Fs_{19–16}$; 0–6 mol% $NaFeSi_2O_6$, 0–1 mol% $NaAlSi_2O_6$, 0–12 mol% $CaFeAlSiO_6$, 0–1 mol% $CaCrAlSiO_6$, 0–1 mol% $CaTiAl_2O_6$, 0–6 mol% $CaAl_2SiO_6$ are present), augite ($Wo_{32–40}En_{43–53}$ $Fs_{11–15}$; 0–4 mol% $NaFeSi_2O_6$, 1–3 mol% $NaAlSi_2O_6$, 0–4 mol% $CaFeAlSiO_6$, 0–1 mol% $CaCrAlSiO_6$, 1–3 mol% $CaTiAl_2O_6$, 5–8 mol% $CaAl_2SiO_6$ are present), and olivine ($Fo_{84}$). These mantle xenocrysts are easily distinguished from the other phenocrysts by their characteristic rounded shape and numerous cracks, but they do not show any deformation features as usually found in mantle xenocrysts.

### Mounts Bambouto

Lavas of this volcano form a differentiation series from basanites to trachytes or phonolites. Three main rock types can be distinguished:

1. Mafic lavas (basanites and basalts) are porphyritic (with up to 30% of phenocryst) or aphyric (<2% microphenocryst). They contain large subhedral phenocrysts of olivine ($Fo_{66–87}$), diopside ($Wo_{45–48}$ $En_{43–52}Fs_{8–17}$; 2–6 mol% $NaFeSi_2O_6$, 0–11 mol% $CaFeAlSiO_6$, 0–3 mol% $CaCrAlSiO_6$, 5–11 mol%

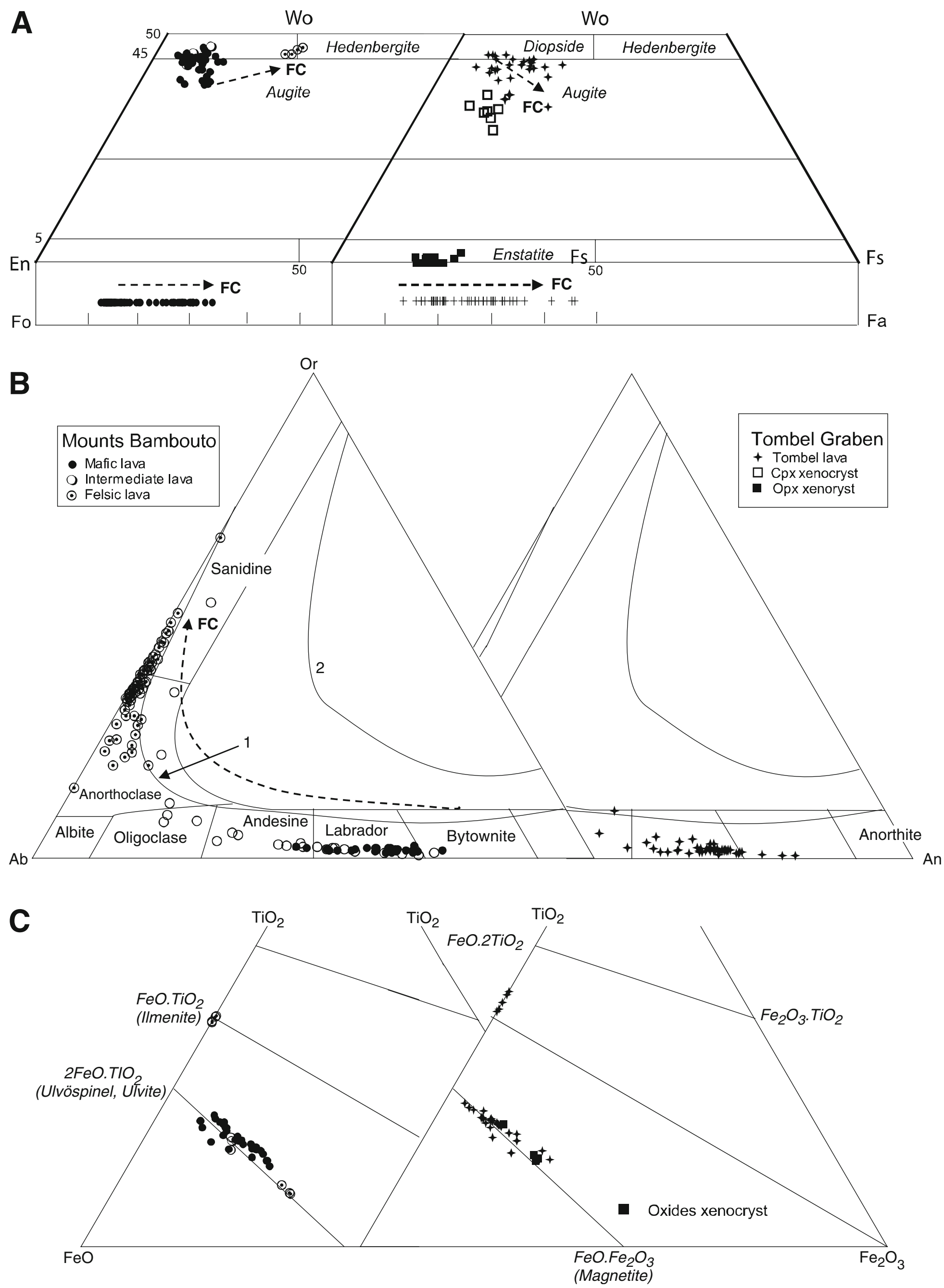


**Fig. 4** **A** Compositions of pyroxenes from Tombel graben (right) and Mounts Bambouto (left) rocks in the enstatite–wollastonite–ferrosilite diagram (mol%) according to Morimoto et al. (1988) and compositions of olivines (forsterite–fayalite in mol%). **B** Feldspar compositions of Tombel graben and Mounts Bambouto volcanic rocks in the Ab–Or–An diagram (mol%). Limits of feldspar solid solutions after Deer et al. (1966). Calculated isothermals solvus sections at 5 kbars and 1,200°C using solid solutions models of (1) Nekvasil and Burnham (1987) and (2) Lindsley and Nekvasil (1989) (both in Nekvasil 1994). **C** Oxide compositions of Tombel graben and Mounts Bambouto rocks in the FeO–$TiO_2$–$Fe_2O_3$ diagram (mol%)

$CaTiAl_2O_6$, 3–11 mol% $CaAl_2SiO_6$ are present), augite ($Wo_{38–44}$ $En_{43–53}Fs_{10–23}$; 4–6 mol% $NaFeSi_2O_6$, 0–2 mol% $NaAlSi_2O_6$, 1–11 mol% $CaFeAlSiO_6$, 0–2 mol% $CaCrAlSiO_6$, 4–12 mol% $CaTiAl_2O_6$, 4–12 mol% $CaAl_2SiO_6$ are present), and scarce phenocrysts and microphenocrysts of plagioclase ($An_{46–72}$) and Fe–Ti oxides (71–19 mol% ulvöspinel). The most magnesian olivines ($Fo_{84–87}$) occur either as large euhedral phenocrysts or as rounded crystals included in larger olivine crystals in more porphyritic basanites, as observed under the microscope, which may indicate them to be xenocrysts. Cr-spinel occurs as scarce small inclusions (<0.2 mm) in olivine phenocrysts or xenocrysts as well as in cpx phenocrysts. Fe–Ti oxides, essentially as microlites, plot along the solid solution line magnetite-ulvöspinel (Fig. 4c) and contain up to 17.4 mol% of spinel $MgAl_2O_4$.

2. Intermediate rocks (hawaiite, phono-tephrite, mugearite) are scarce, as has been observed in other series of the CVL and elsewhere in Africa (Ethiopia, Peccerillo et al. 2003, 2007; Tchad, Gourgaud and Vincent 2004; Sudan, Franz et al. 1999). They contain mainly phenocrysts and microphenocrysts of plagioclase ($An_{12–70}$; Fig. 4b) associated with variable amounts of diopsidic

**Table 2** Whole rock compositions of representative Tombel and Bambouto lavas

| | Tombel | | | | | | | | | Bambouto | | | | | | | | | | | | | |
|---|---|---|---|---|---|---|---|---|---|---|---|---|---|---|---|---|---|---|---|---|---|---|---|
| | NT19 | NT39 | NT30 | TPL1 | NT15 | EM2 | TLC1 | NT34 | NT25 | NG6 | BL4 | MM1 | FR1 | CB3 | KBP-5 | BL2 | DB1 | CB1a | CB2 | Ant1 | DJ1 | Kh1 | NG3 |
| | Ba | Bas | Bas | Bas | Bas | Haw | Haw | Haw | Haw | Bas | Bas | Bas | Bas | Bas | Bas | Bas | Bas | Pht | Mug | Ben | Trach | Trach | Phono |
| Major elements (wt%) | | | | | | | | | | | | | | | | | | | | | | | |
| $SiO_2$ | 43.70 | 48.59 | 47.29 | 45.22 | 46.53 | 44.64 | 47.05 | 46.92 | 48.85 | 43.56 | 41.41 | 42.83 | 44.61 | 46.20 | 41.34 | 42.45 | 44.19 | 50.63 | 51.46 | 56.51 | 62.73 | 58.74 | 60.96 |
| $Al_2O_3$ | 12.44 | 15.40 | 15.57 | 15.48 | 16.09 | 15.01 | 15.96 | 17.02 | 17.39 | 15.58 | 11.67 | 13.97 | 15.91 | 16.32 | 10.72 | 13.50 | 12.88 | 17.59 | 16.44 | 17.22 | 14.26 | 18.84 | 16.98 |
| $Fe_2O_3$ | 12.67 | 12.88 | 12.55 | 14.13 | 13.26 | 14.07 | 13.25 | 13.68 | 12.64 | 13.34 | 12.90 | 14.33 | 13.52 | 12.09 | 13.86 | 13.65 | 12.28 | 9.90 | 9.62 | 8.12 | 6.55 | 5.11 | 6.27 |
| MnO | 0.18 | 0.14 | 0.15 | 0.21 | 0.19 | 0.20 | 0.18 | 0.15 | 0.16 | 0.19 | 0.18 | 0.17 | 0.20 | 0.21 | 0.20 | 0.17 | 0.18 | 0.24 | 0.24 | 0.24 | 0.42 | 0.27 | 0.43 |
| MgO | 11.73 | 6.56 | 7.13 | 5.18 | 7.10 | 7.65 | 6.63 | 5.07 | 4.01 | 6.38 | 14.43 | 9.29 | 5.88 | 4.89 | 15.28 | 10.17 | 12.15 | 2.28 | 2.16 | 1.82 | 0.60 | 0.64 | 0.07 |
| CaO | 11.33 | 8.67 | 9.23 | 9.21 | 9.20 | 9.48 | 9.43 | 7.76 | 6.86 | 9.17 | 10.67 | 10.59 | 8.57 | 9.22 | 10.00 | 11.02 | 9.67 | 6.42 | 5.87 | 4.20 | 0.54 | 1.90 | 0.81 |
| $Na_2O$ | 2.70 | 3.60 | 3.28 | 3.29 | 3.65 | 3.79 | 3.60 | 4.01 | 4.71 | 2.88 | 2.58 | 2.15 | 3.37 | 4.34 | 3.16 | 3.09 | 3.16 | 5.76 | 4.89 | 5.00 | 5.44 | 7.40 | 6.77 |
| $K_2O$ | 0.81 | 0.95 | 1.06 | 1.09 | 1.51 | 1.63 | 1.35 | 1.19 | 1.58 | 1.74 | 0.93 | 1.41 | 1.79 | 1.68 | 0.61 | 1.07 | 1.19 | 2.41 | 2.61 | 2.99 | 5.58 | 5.00 | 4.77 |
| $TiO_2$ | 2.67 | 2.81 | 2.71 | 3.48 | 2.80 | 3.14 | 3.31 | 3.32 | 2.72 | 4.25 | 2.80 | 4.11 | 4.09 | 2.93 | 2.65 | 3.53 | 2.72 | 1.93 | 1.88 | 1.21 | 0.64 | 0.30 | 0.10 |
| $P_2O_5$ | 0.65 | 0.45 | 0.47 | 0.94 | 0.55 | 0.71 | 0.51 | 0.57 | 0.74 | 0.76 | 0.83 | 0.50 | 0.91 | 1.26 | 0.88 | 1.01 | 0.71 | 0.93 | 1.03 | 0.85 | 0.12 | 0.14 | 0.07 |
| LOI | 0.94 | 0 | 0.33 | 0 | 0.00 | 0.00 | 2.52 | 1.65 | 0.58 | 1.66 | 1.21 | 1.06 | 0.36 | 0.92 | 2.02 | 3.33 | 1.49 | 3.07 | 2.04 | 3.20 | | | 3.20 |
| Total | 97.76 | 98.91 | 98.33 | 96.98 | 99.71 | 99.08 | 100.10 | 98.48 | 98.54 | 100.36 | 100.05 | 99.93 | 100.50 | 100.34 | 99.75 | 100.02 | 100.05 | 100.10 | 99.54 | 99.65 | 99.95 | 100.38 | 100.42 |
| Quartz | – | – | – | – | – | – | – | – | – | – | – | – | – | – | – | – | – | – | – | 2.20 | 5.55 | – | – |
| Neph. | 7.14 | – | 0.82 | 0.89 | 6.08 | 10.20 | 4.29 | 2.23 | 2.98 | 3.83 | 10.19 | 4.39 | 4.18 | 7.77 | 12.06 | 9.71 | 8.11 | 7.76 | 0.10 | – | – | 10.49 | 0.23 |
| Hyp. | – | 2.17 | – | – | – | – | – | – | – | – | – | – | – | – | – | – | – | – | – | 14.32 | 9.68 | – | – |
| DI | 22.22 | 36.47 | 33.90 | 34.60 | 34.78 | 33.46 | 34.77 | 39.71 | 47.39 | 32.59 | 19.48 | 23.33 | 36.49 | 41.06 | 20.90 | 24.76 | 27.59 | 58.20 | 59.51 | 63.74 | 83.66 | 85.31 | 88.25 |
| mg# | 0.68 | 0.53 | 0.56 | 0.45 | 0.55 | 0.55 | 0.53 | 0.45 | 0.42 | 0.52 | 0.72 | 0.59 | 0.49 | 0.48 | 0.71 | 0.63 | 0.69 | 0.34 | 0.34 | 0.33 | 0.18 | 0.22 | 0.03 |
| **Trace elements ppm (μg/g)** | | | | | | | | | | | | | | | | | | | | | | | |
| Ba | 387.00 | 257.00 | 367.00 | 463.70 | 410.50 | 488.00 | 398.30 | 409.00 | 520.00 | 394.50 | 572.40 | 300.70 | 449.90 | 920.90 | 567.30 | 626.70 | 648.30 | 1147.00 | 996.40 | 917.20 | 46.05 | 300.60 | 18.88 |
| Ce | 72.17 | 55.28 | 65.88 | 92.86 | 91.17 | 116.60 | 79.23 | 80.27 | 104.00 | 107.40 | 80.97 | 79.46 | 126.30 | 99.82 | 77.56 | 75.13 | 72.55 | 117.10 | 153.80 | 196.30 | 351.10 | 180.40 | 432.10 |
| Co | 51.60 | 39.20 | 42.70 | 35.49 | 43.53 | 45.09 | 47.05 | 36.80 | 27.60 | 41.59 | 57.46 | 56.52 | 37.65 | 31.32 | 62.80 | 52.53 | 54.22 | 15.26 | 8.63 | 7.81 | 2.02 | 2.46 | <L.D. |
| Cr | 508.00 | 181.00 | 163.00 | 44.52 | 119.50 | 159.00 | 122.00 | 12.10 | <L.D. | 47.07 | 661.00 | 302.40 | 8.78 | 71.60 | 860.10 | 292.40 | 771.40 | 8.01 | <L.D. | <L.D. | <L.D. | <L.D. | <L.D. |
| Eu | 2.35 | 2.60 | 2.43 | 3.81 | 2.69 | 3.80 | 2.83 | 3.02 | 3.47 | 3.19 | 2.73 | 2.73 | 3.52 | 3.37 | 2.58 | 2.98 | 2.65 | 3.18 | 4.83 | 4.29 | 2.59 | 0.92 | 2.32 |
| Hf | 4.27 | 4.94 | 5.28 | 4.88 | 5.94 | 7.90 | 5.78 | 6.30 | 7.44 | 7.09 | 3.93 | 5.71 | 7.78 | 5.41 | 3.79 | 4.04 | 4.27 | 7.11 | 9.37 | 13.24 | 26.28 | 23.43 | 49.88 |
| La | 34.65 | 24.29 | 31.35 | 44.40 | 44.85 | 57.44 | 38.00 | 38.38 | 51.07 | 51.94 | 39.73 | 35.62 | 60.09 | 49.71 | 38.84 | 35.28 | 34.28 | 61.09 | 73.06 | 96.01 | 179.60 | 115.10 | 259.60 |
| Lu | 0.21 | 0.31 | 0.27 | 0.30 | 0.30 | 0.52 | 0.32 | 0.32 | 0.37 | 0.35 | 0.23 | 0.28 | 0.37 | 0.33 | 0.23 | 0.23 | 0.25 | 0.39 | 0.42 | 0.59 | 1.14 | 0.86 | 1.35 |
| Nb | 46.50 | 35.60 | 41.30 | 49.65 | 58.46 | 77.78 | 54.67 | 52.30 | 66.70 | 73.33 | 54.14 | 48.69 | 81.80 | 62.51 | 53.48 | 43.68 | 46.58 | 88.20 | 85.09 | 106.00 | 226.70 | 196.50 | 457.50 |
| Nd | 35.46 | 31.30 | 32.94 | 47.06 | 41.89 | 57.51 | 40.15 | 40.80 | 51.42 | 52.94 | 40.13 | 41.61 | 59.87 | 50.66 | 38.37 | 40.90 | 37.68 | 51.34 | 72.14 | 85.17 | 132.20 | 49.38 | 126.60 |
| Ni | 272.00 | 97.60 | 79.80 | 31.03 | 89.36 | 120.00 | 74.23 | 28.90 | 6.38 | 62.08 | 311.40 | 131.70 | 30.28 | 33.36 | 392.20 | 148.60 | 275.80 | 5.71 | <L.D. | <L.D. | <L.D. | <L.D. | <L.D. |
| Pb | 3.22 | 1.65 | 2.17 | 1.97 | 2.86 | 4.70 | 4.02 | 2.41 | 2.98 | 2.56 | 1.75 | 2.15 | 2.91 | 3.04 | 1.91 | 1.49 | 1.21 | 5.23 | 4.41 | 6.83 | 17.74 | 26.63 | 41.36 |
| Pr | 8.68 | 6.86 | 7.71 | 11.29 | 10.60 | 13.54 | 9.90 | 9.50 | 11.90 | 13.28 | 9.73 | 9.92 | 15.32 | 12.44 | 9.40 | 9.53 | 8.98 | 13.54 | 18.49 | 22.70 | 38.62 | 16.47 | 41.65 |
| Rb | 24.40 | 17.60 | 22.10 | 16.71 | 33.66 | 41.96 | 27.55 | 18.60 | 26.00 | 52.63 | 29.60 | 30.27 | 33.99 | 37.57 | 47.17 | 23.05 | 27.32 | 58.90 | 49.96 | 64.56 | 106.10 | 247.60 | 258.40 |
| Sm | 7.66 | 7.41 | 7.12 | 9.92 | 8.36 | 12.18 | 8.51 | 8.75 | 10.37 | 10.23 | 8.03 | 8.61 | 11.21 | 9.69 | 7.59 | 8.43 | 7.57 | 9.23 | 13.17 | 14.66 | 22.39 | 7.57 | 20.88 |
| Sr | 669.00 | 502.00 | 596.00 | 847.00 | 694.00 | 767.00 | 749.40 | 721.00 | 856.00 | 888.50 | 929.20 | 636.70 | 1053.00 | 1277.00 | 931.00 | 1133.00 | 968.40 | 1248.00 | 1148.00 | 924.80 | 13.55 | 227.90 | 14.72 |
| Ta | 3.23 | 2.63 | 3.01 | 3.66 | 4.24 | 6.04 | 3.89 | 3.90 | 4.78 | 5.41 | 4.00 | 3.73 | 5.97 | 4.59 | 3.79 | 3.17 | 3.50 | 6.41 | 6.35 | 7.80 | 15.93 | 16.36 | 40.50 |
| Tb | 0.88 | 1.04 | 0.90 | 1.20 | 1.03 | 1.47 | 1.09 | 1.12 | 1.26 | 1.15 | 0.92 | 1.03 | 1.25 | 1.13 | 0.88 | 0.97 | 0.88 | 1.03 | 1.38 | 1.56 | 2.66 | 1.03 | 2.66 |
| Th | 3.47 | 2.21 | 3.21 | 3.74 | 4.88 | 7.16 | 3.77 | 3.92 | 4.95 | 5.13 | 4.23 | 3.59 | 5.66 | 4.58 | 4.01 | 3.38 | 3.47 | 7.20 | 7.08 | 10.84 | 23.39 | 37.14 | 64.68 |
| Y | 22.70 | 26.60 | 23.20 | 30.23 | 26.66 | 30.44 | 28.84 | 28.00 | 32.00 | 29.55 | 22.34 | 25.78 | 31.66 | 28.55 | 21.51 | 22.61 | 21.67 | 28.57 | 34.37 | 42.40 | 80.81 | 41.63 | 86.98 |
| Zr | 192.00 | 189.00 | 211.00 | 204.80 | 261.60 | 330.00 | 254.40 | 262.00 | 326.00 | 327.80 | 172.10 | 244.00 | 369.60 | 238.20 | 166.80 | 171.10 | 187.80 | 344.00 | 458.90 | 623.80 | 1238.00 | 1122.00 | 2033.00 |

Major and trace elements were determined by ICP-OES and ICP-MS at CRPG at Nancy, France.
*Ba* Basanite, *Bas* basalte, *Haw* hawaiite, *Pht* phonotephrite, *Mug* mugearite, *Ben* benmoreite, *Trach* trachyte, *Phono* phonolite, *mg#* [Mg/(Mg+$Fe^{2+}$)]

augite ($Wo_{43-48}En_{47-51}Fs_{10-15}$; 4–8 mol% $NaFeSi_2O_6$, 1–9 mol% $CaFeAlSiO_6$, 7–14 mol% $CaTiAl_2O_6$, 4–5 mol% $CaAl_2SiO_6$ are present), Ca-amphibole (edenite and kaersutite) and Fe–Ti oxides (titanomagnetite with 57–41 mol% ulvöspinel, and ilmenite, Fig. 4c). The same minerals occur in mugearites as matrix phases embedded in the groundmass (5–15% glass) with scarce sanidine ($Or_{45-65}Ab_{35-55}An_{0-6}$; Fig. 4b).

3. Felsic lavas (benmoreite, trachyte, phonolite) tend to have a trachytic texture. Feldspars (anorthoclase $An_{25-11}$ $Ab_{70-54}Or_{22-19}$ and alkali feldspar, i.e. sanidine to Na-sanidine, $Or_{15-55}Ab_{35-85}An_{0-6}$) constitute the main phenocrysts in a microlitic matrix of alkali feldspar, plagioclase, cpx and titanomagnetite (94–25 mol% ulvöspinel). They are also characterised by sodic cpx ($En_{3-4}Aeg_{33-35}Fs_{62-65}$) or hedenbergite ($Wo_{45-47}En_{26-30}$ $Fs_{40-44}$; Fig. 4a). Njonfang and Nono (2003) argued that the evolution of pyroxenes from calcic to sodic composition is linked to increasingly oxidized conditions at the end of crystallization.

In some phonolite samples, scarce nepheline ($Na_{2.9-3.0}$ $K_{0.3-0.4}Al_{3.3-3.5}Si_{4.5-4.6}O_{16}$) and sodalite ($Na_{7.5-7.6}Al_{5.7-6.0}$ $Si_{6.0-6.2}O_{24}Cl_{1.9-2.0}$) are observed, however, locally completely pseudomorphed by alteration products. Feldspar ($An_{0-1}Ab_{62-85}Or_{15-46}$) crystals are optically zoned: both normal zoning and occasional reverse zoning are observed. Their rims reach more sodic compositions ($An_{11}Ab_{70}Or_{19}$) and correspond to the crystals of the groundmass, which are mainly microlites and skeletal microphenocrysts.

Ignimbrites, of trachytic or more rarely rhyolitic composition, are also very common and widespread in the Mounts Bambouto region. These rocks generally contain complete or broken crystals of alkali feldspar associated with variable amounts of plagioclase, quartz, biotite and cpx, and distorted fiamme in a devitrified matrix consisting of fine rods of alkali feldspar and quartz (pseudomorphs after cristobalite) crystallites (Nono et al. 2004). Subangular and rounded fragments of scoria are observed. Occurrence of enclaves of trachyte and granitic basement argues for some contamination (see below).

### Evolutionary trend

The morphology, mutual relationships and chemistry of the different minerals (both phenocrysts and microlites) of the lavas of these two regions generally follow an evolutionary trend, from mafic to more evolved composition, but with no apparent relationship to age data (Fig. 3). Chemical compositions of pyroxenes and olivines (Fig. 4a) show Fe-enrichment with differentiation. Moreover, some lavas of Mounts Bambouto horst may result from some slight amounts of magma mixing as indicated by the reverse zoning of some feldspars (exceptionally clinopyroxenes) as well as resorption that occurred in clinopyroxene but also in feldspars. The different components of this mixing were probably magmas with similar chemical composition, more or less differentiated, inside a small zoned magma reservoir.

We used the geobarometer of Nimis and Ulmer (1998) on clinopyroxene phenocrysts to obtain a quantitative estimation of the pressure during formation of the Tombel graben and Mounts Bambouto magmas. This barometer is recommended by the authors for near-liquidus cpx. The calculated pressures for Tombel graben are 0 to 0.3 kbar for the Upper Volcanic Unit (UVU), 1–2 kbar for the Lower Volcanic Unit (LVU), and 6–8.5 kbar for xenoliths. For such calculations, the estimated standard error is 1.7 kbar. Therefore, the crystallization scenario shown by the clinopyroxene geobarometer clearly reflects different storage zones of magmas in Tombel graben volcanoes: (1) near the surface (UVU), (2) in a shallow reservoir (LVU), (3) the high pressures calculated for xenolith phases represent early-formed mantle minerals at depths of ~25–27 km, which then moved upwards with the ascending magma.

According to the same geobarometer, pressures are 1–4 kbar for mafic lavas of Mounts Bambouto, independent of their age. These calculated pressures indicate crystallization at upper crustal levels in a large magma chamber. No pyroxene xenocrysts are found in Mounts Bambouto. The diopsides in basanites crystallized at a deeper level.

This rather wide pressure range argues for more complex processes than those discussed by Sato et al. (1990) who stated that all the basalts of the CVL were formed at a similar depth from rather similar peridotitic rocks under vapor saturated conditions. The rather wide pressure range that we have calculated indicate that, if the balsaltic magmas have formed by partial melting of mantle rocks at about the same depth(s), the phenocrysts crystallized in magma chambers at shallower, but different levels.

## Geochemistry and magma genesis

Compositions of selected representative bulk-rock analyses are presented in Table 2.

### Major elements

1. Series. Tombel graben and Mounts Bambouto basic lavas are silica-undersaturated with CIPW-normative nepheline ranging between 0 and 13 wt%. The diagram of total alkalis ($Na_2O+K_2O$) vs $SiO_2$ (Fig. 5) shows that from the rocks investigated, basanites seem to be abundant in Mounts Bambouto but scarce in Tombel graben; basalts of Tombel graben are mildly alkaline and have rather

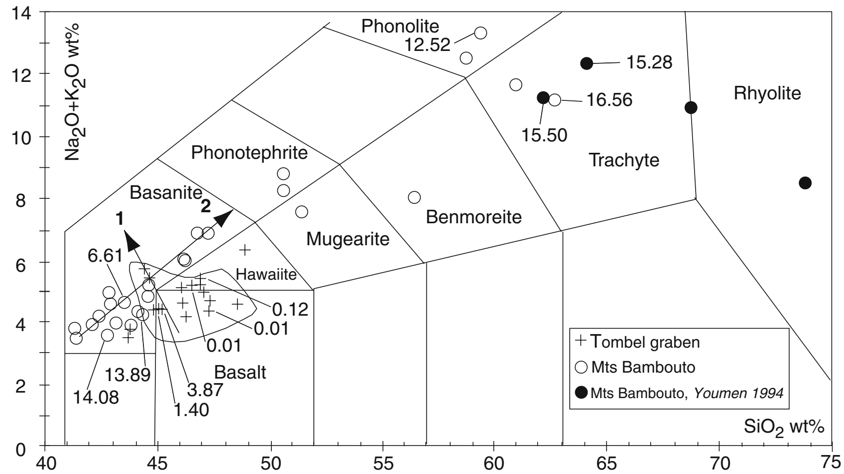


**Fig. 5** Total alkalis versus silica diagram showing the composition range and evolution trend of Tombel graben and Mounts Bambouto lavas (rock classification from Le Maitre 2002). *1* Evolution by increasing rate of partial melting, *2* Evolution by fractional crystallization following Guille et al. (1993). K-Ar ages (see Table 1) are indicated. New data, except pyroclastic rocks (ignimbrites) of Bambouto after Youmen (1994)

higher contents of $SiO_2$ while those of Mounts Bambouto are alkaline to peralkaline with less silica.

The trend of lavas of Mounts Bambouto shows a large variation with systematic increase in $SiO_2$, $K_2O$ and $Na_2O$, and decrease of MgO, FeO and CaO as well as Cr and Ni (Fig. 6), indicating that fractional crystallisation of olivine, clinopyroxene and Ca-plagioclase was the main process responsible for the more evolved rocks. Some of the evolved lavas of Mounts Bambouto, like the benmoreites and quartz-trachytes (analysis DJ1, Table 2), are weakly oversaturated (with 2–6 wt% normative quartz). In contrast, the Tombel graben series is far less differentiated.

2. Primary magmas. Some basalts of both Tombel graben and Mounts Bambouto have geochemical features [MgO>10 wt%, Cr>500 ppm, Ni>200 ppm, mg#>68, with mg#=100 Mg/(Mg+Fe)] typical of more or less primary magmas derived from a peridotitic source. Ultramafic mantle xenoliths are more common in Tombel graben lavas. According to silica and alkali contents, the basalts of Tombel graben may result from higher rates of partial melting than those of Mounts Bambouto. Contamination may have played only a minor role (see below). Moreover, melting under low $CO_2/H_2O$ ratios produced only slightly undersaturated basalts (according to Sato et al. 1990) of monogenetic volcanoes as in Tombel graben. Meanwhile, melting under higher $CO_2/H_2O$ ratios produced higher degree undersaturated basalts (compared to Tombel graben basalts) of polygenetic volcanoes as in Mounts Bambouto.

## Trace elements

In primitive-mantle-normalized multi-element variation diagrams (Fig. 7), trace element patterns are strongly parallel and suggest more or less a common basaltic source. All mafic lavas have high abundances of LREE. All display trends of typical alkaline rocks with negative K, Rb anomalies. However, some trace element ratios of basalts from the two environments differ slightly; for example Ba contents are higher in Mounts Bambouto rocks. These features could confirm that the basalts were derived from two slightly different parental magmas. For comparison, note that the HIMU pattern from Polynesia (Fig. 7) is rather parallel to that of both Tombel graben and Mounts Bambouto suggesting an identical source composition with typical OIB sources.

Low values of HREE in primitive mantle-normalized multi-element variation diagrams (spidergrams) can be interpreted as the result of the presence of a minor amount of garnet in the mantle source. The basalts of the two sectors suggest an origin in a nearly uniformly enriched mantle source (Nkouathio et al. 2006). They could have been generated by a low rate of partial melting of a metasomatised garnet lherzolite perhaps with some amphibole. This could account for the distinct depletions of elements such as Rb or Yb, as described by Wilson and Downes (1991) and Gourgaud and Vincent (2004).

Figure 8 illustrates the differences between the processes of partial melting between the two basalts using the $(Ce/Sm)_N$ vs $Ce_N$ diagram. We observe that the basalts of the two regions have slightly different trends. Assuming that the partition coefficients are the same for both lavas, the models for magma generation in these regions indicate a very small difference of source composition and are consistent with a range in partial melting of around 1.5–3% for the lavas of Tombel graben and around 0.5–3% for those of Mounts Bambouto (Fig. 8). This is illustrated by the calculated liquid composition for $(Ce/Sm)_N$ vs $Ce_N$ formed by partial melting of supposedly primary mantle source (according to formula of Rollinson (1993): $C_L/C_O=1/[D_O+F(1-D_O)]$ where $D_O$ is the bulk partition coeffi-

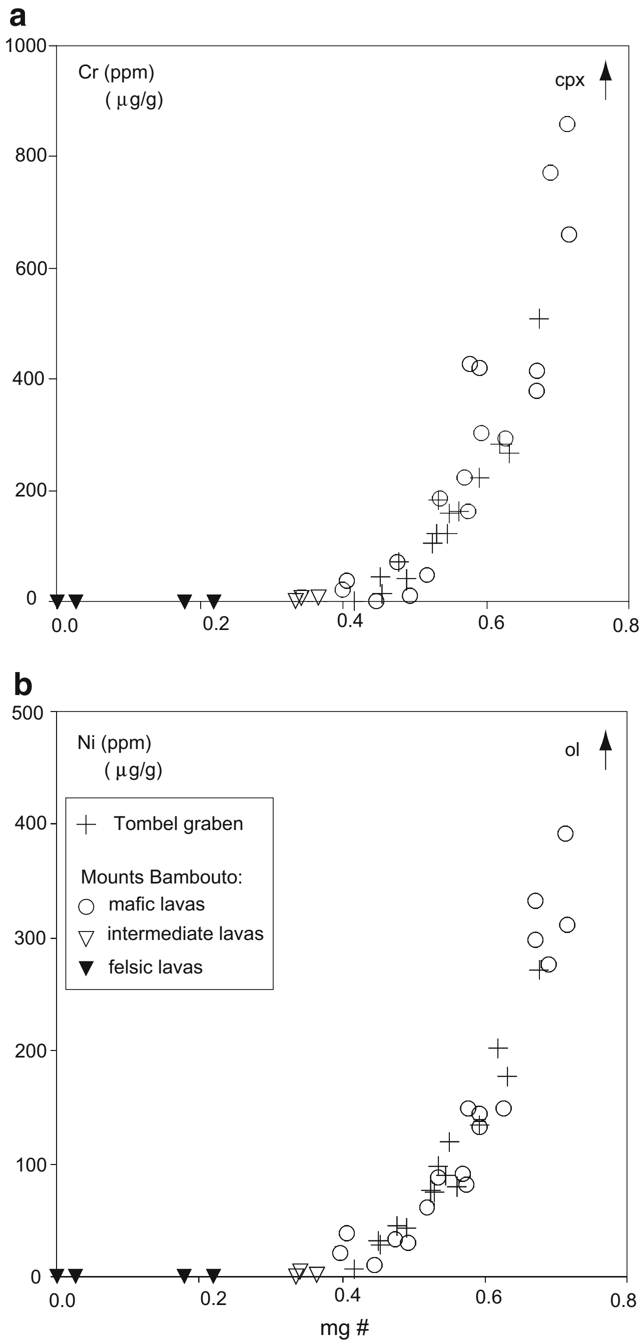


**Fig. 6** Cr and Ni contents vs. mg#[=Mg/(Mg+$Fe^{2+}$)]. Clinopyroxenes (*cpx*) of Tombel and Mounts Bambouto often contain 1,000–2,000 and up to 5,000 ppm of Cr for mg# ranging between 0.7 and 0.8; Olivines (*ol*) of Tombel graben contain 1,500–3,000 ppm of Ni for Fo ranging between 0.65 and 0.85 while olivines of Mounts Bambouto contain 1,000–2,500 ppm of Ni for Fo ranging between 0.75 and 0.85

cient). Figure 8 indicates a slight increase in $(Ce/Sm)_N$ ratios with the progress of melting from Tombel graben to Mounts Bambouto. After partial melting of a garnet lherzolite mantle source, fractional crystallization was the main differentiation process for the two suites. Major and trace element distribution suggest that fractional crystallization is the dominant process for generation of intermediate and felsic lavas from a basanitic parental magma. The petrographic and mineralogical study indicates the early crystallization of olivine and Cr-spinel, probably preceded by Ca-clinopyroxene at the early stage, followed by plagioclase and Fe–Ti oxides and amphiboles. Na-clinopyroxene, Na-plagioclase and alkali feldspar crystallised as the last major phase in Mounts Bambouto, with feldspathoids as minor phases essentially in phonolite. Note that the volume of felsic lava flows is estimated at 6.5 $km^3$ and the volume of felsic ignimbritic flows at 1.5 $km^3$, that is not so important in comparison to the huge volume of basic rocks. From all the diagrams, there is no evidence of any magma mixing between very primitive and more evolved compositions. This does not exclude the possibility of mixing of relatively evolved magma inside a simple zoned magma chamber as suggested by petrographical observations.

La/Nb vs. Zr/Nb ratios (Fig. 9a) as well as some other ratios (Table 3) show that all lavas from both Tombel graben and Mounts Bambouto present characteristics similar to rocks which could have originated from HIMU and enriched mantle (EM).

All these basalts have LOI<2% argues for only slight weathering. Note, however, that NG6 sample from Mounts Bambouto has a LOI of 2.52 wt%; some trace elements are high in that lava (especially Ta, Zr, Hf, Ti). Rather high contents of some elements, such as Rb, U, Th could indicate that crustal contamination may have played some role.

For the Meidob Hills Volcanic Field in Darfur, Sudan, which displays a complete series from basalts to both phonolites as well as benmoreites and trachytes, Franz et al. (1997, 1999) described significant crustal contamination in benmoreitic–trachytic rocks. This is evidenced by both high Ba (1,000–1,800 ppm) and rather low Sr (less than 500 ppm) contents. Some of the rocks of Mounts Bambouto have rather high Ba contents (up to 1,150 ppm, Fig. 10a, Table 2) but Sr contents are also high (up to 1,330 ppm). A peculiar plagioclase-rich sample (KWA-2) contains 1,584 ppm Ba and 1,829 ppm Sr (Fig. 10a). Thus, it appears that contamination does not play a major role in Tombel graben and Mounts Bambouto but does exist according to petrographical observations (see above). The fractionations of olivine and pyroxene clearly increase Sr and Ba contents of the residual liquid (Fig. 10a). The role of plagioclases is more complex. Some plagioclases (essentially the Ca-richest) are Sr- and Ba-poor (less than 500 ppm) and their fractionations increase Sr and Ba contents of the residual liquid. Reversely, other plagioclases (essentially the Ca-poorest), which are Sr- and Ba-rich (up to 3,000 ppm), produce the opposite effect.

Conversely, the Zr/Nb vs Zr diagram (Fig. 10b) argues for more assimilation for some samples, such as CB2 (mugearite) and Ant1 (benmoreite) of Mounts Bambouto which have

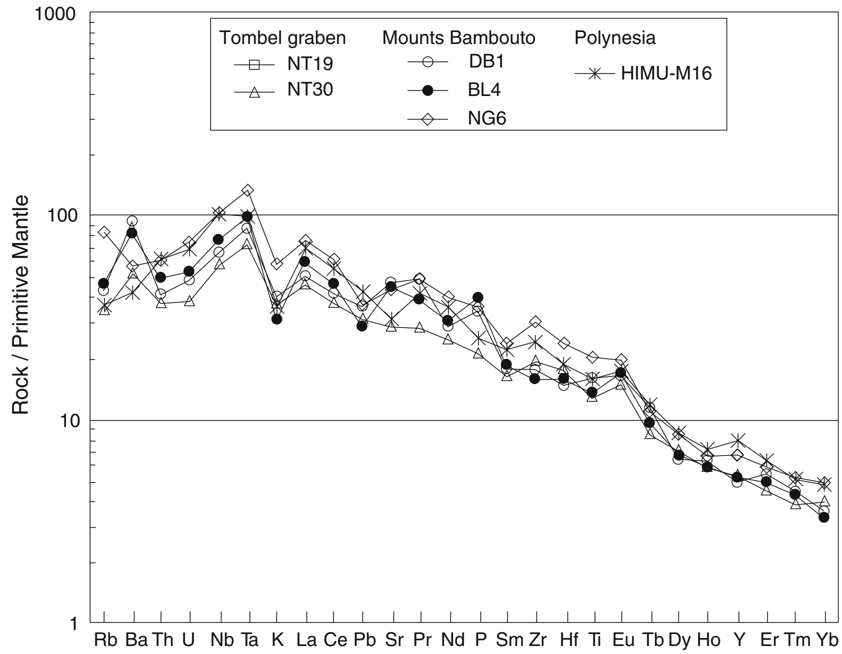


**Fig. 7** Primitive mantle-normalized spidergrams for incompatible elements for selected mafic lavas of Tombel graben and Mounts Bambouto horst compared with HIMU. Normalizing values after Sun and McDonough (1989)

high Zr/Nb ratios of 5.4 and 5.9 respectively for medium Zr contents of 459 and 624 ppm. By contrast, trachyte samples display considerably higher Zr values of 1,122 and 1,238 ppm, and phonolite contains even 2,033 ppm Zr (Table 2), clearly indicating a fractionation process.

## Isotopic data

A mantle origin of the lavas is confirmed by Sr and Nd isotopic ratios (five new analyses in this work for Tombel graben and Mounts Bambouto, Table 4), conforming to the range of data obtained for the Mounts Bambouto lavas and other massifs of CVL (Halliday et al. 1990; Lee et al. 1994; Marzoli et al. 2000; Fig. 9b). They plot in the same representative field of Ahaggar alkaline rocks (Aït-Hamou et al. 2000). Lavas of Tombel graben and Mounts Bambouto have Sr, Nd isotopic compositions similar to those of the neighbouring island of Sainte Helena which has been shown to have a typical HIMU (high $\mu$ with $\mu={}^{238}U/{}^{204}Pb$) composition (Zindler and Hart 1986; Hart 1988; Weaver 1991). For Tombel graben, $^{87}Sr/^{86}Sr$ varies between 0.70342 and 0.70364 and $^{143}Nd/^{144}Nd$ from 0.512873 to 0.512933. In comparison, mafic lavas from Mounts Bambouto volcano have $^{87}Sr/^{86}Sr$ compositions ranging from 0.703248 to 0.70425 and $^{143}Nd/^{144}Nd$ from 0.512859 to 0.512863. All these values are close to those of HIMU but some data of Lee et al. (1994) and Marzoli et al. (2000) for Mounts Bambouto indicate minor contribution of DMM (depleted mantle) and EM1 (enriched mantle) mantle components (Fig. 9b, Table 4).

Most of the representative values plot in a domain very close to FOZO (focal zone) as recently redefined (Stracke et al. 2005) according to significantly more radiogenic Sr isotope signatures (Fig. 9b). A FOZO mantle component could better explain the genesis of Tombel graben and Mounts Bambouto rocks, as pointed out by Déruelle et al.

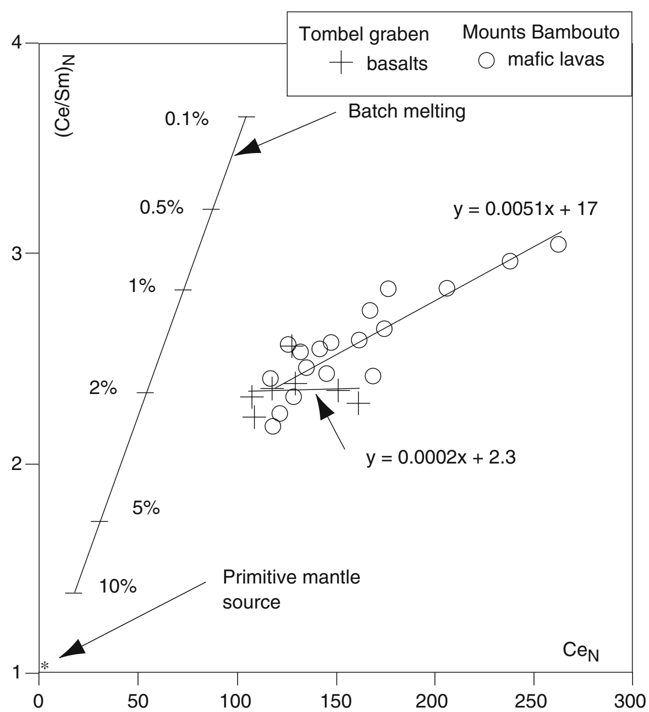


**Fig. 8** $(Ce/Sm)_N$ vs $Ce_N$ plot showing degrees of partial melting, assuming fractional melting of a primitive mantle source (with the melting reaction: $C_L/C_O=1/[D_O+F(1-D_O)]$, where $D_O$ is the bulk partition coefficient, following Rollison (1993) and Kil (2007)) composed of 55 wt % olivine, 25 wt% cpx, 11 wt% opx, 9 wt% garnet. Regression lines should only be taken as indicators of trends because of the scatter of the data

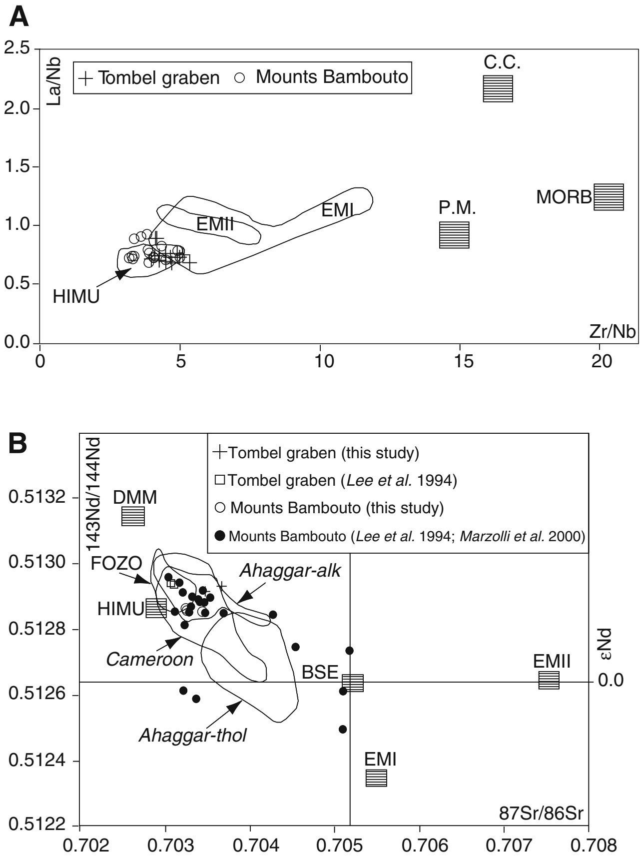


**Fig. 9** **A** La/Nb vs Zr/Nb diagram for lavas from Tombel graben and Mounts Bambouto horst. Composition fields for HIMU, EMI, EMII, Primitive Mantle (*P.M.*), Mid-Oceanic Ridge Basalt (*MORB*), Continental Crust (*C.C.*) from Weaver (1991). HIMU and EM as defined in Table 4. **B** $^{143}$Nd/$^{144}$Nd vs $^{87}$Sr/$^{86}$Sr diagram showing the range of isotopic compositions measured for Mounts Bambouto and Tombel graben lavas. Composition of Depleted-MORB Mantle (*DMM*), HIMU, EMI and EMII are from Faure (2001), Bulk Silicate Earth (*BSE*) after Allègre (2005), FOcal ZOne (*FOZO*) after Stracke et al. (2005). Field of lavas of Mount Cameroun and Mount Manengouba in Cameroon (Halliday et al. 1990) as well as fields of tholeiite and alkaline lavas of Ahaggar (Taharaq) lavas (Aït-Hamou et al. 2000) are drawn for comparison

(2007) for the whole Cameroon Volcanic Line. However DMM and EMI poles could have played a role too.

These lavas have geochemical and isotopic signatures close to OIB, implying the contribution of at least several components: FOZO and other components as DMM and EMI, especially for some rocks of Mounts Bambouto (Fig. 9).

## Conclusions

Field investigations, age determinations, petrographical and geochemical data were used to describe the development of Tombel graben and Mounts Bambouto horst. These main volcanoes contain characteristics of all volcanoes of the central continental part of CVL. We assume that Tombel graben is a volcanic field, consisting of typical monogenetic volcanoes, as defined by von Wolff (1914) and Walker (2000), in a trough, and Mounts Bambouto is a typical central polygenetic volcano on a horst. In CVL, they also represent young and old volcanoes, respectively.

Age determinations attest to several periods of magmatic activity separated by periods of quiescence for Tombel graben. For Mounts Bambouto only one discrete period of quiescence is evident (Fig. 3a,b). Magmatism of Tombel graben appears to follow the graben forming tectonic activity (post-tectonic) while magmatism of Mounts Bambouto is both syn-tectonic and post-tectonic relative to the horst formation.

More generally, magmatism of the CVL is linked to the Central Cameroon Shear Zone (Fig. 1b) and, at a greater scale, to the Central African Fault Zone which is developed from Cameroon to Chad, Central African Republic until Sudan. Franz et al. (1999) emphasized the important role played by this megastructure for the igneous activity in the Darfur Dome in Sudan, i.e. not for magma generation but for the ascent of the magma. Zones of weakness and brittle

**Table 3** Incompatible trace-element ratios of mafic lavas from Tombel graben and Mounts Bambouto (Nkouathio 2006) compared with different OIB components and other mantle and crustal reservoirs

| | Zr/Nb | La/Nb | Ba/Nb | Ba/Th | Rb/Nb | K/Nb | Th/Nb | Th/La | Ba/La |
|---|---|---|---|---|---|---|---|---|---|
| Chondrite | 15.7 | 0.96 | 9.8 | 83 | 9.4 | 2215 | 0.117 | 0.122 | 10.16 |
| Primitive mantle | 14.8 | 0.94 | 9 | 77 | 0.91 | 323 | 0.117 | 0.125 | 9.6 |
| N. MORB | 30 | 1.07 | 4.3 | 60 | 0.36 | 296 | 0.071 | 0.067 | 4 |
| Continental crust | 16.2 | 2.2 | 54 | 124 | 4.7 | 1341 | 0.44 | 0.204 | 25 |
| Average OIB | 5.8 | 0.77 | 7.3 | 88 | 0.64 | 250 | 0.083 | 0.108 | 9.4 |
| HIMU | 3.2–5 | 0.66–0.77 | 4.9–6.5 | 49–77 | 0.35–0.38 | 77–179 | 0.078–0.101 | 0.107–0.133 | 6.9–8.7 |
| EMI | 4.2–11.4 | 0.64–1.19 | 11.4–17.7 | 103–154 | 0.88–1.17 | 204–432 | 0.105–0.122 | 0.107–0.128 | 13.2–16.9 |
| EMII | 4.5–7.3 | 0.89–1.09 | 7.3–11 | 67–84 | 0.59–0.85 | 248–378 | 0.111–0.157 | 0.122–0.163 | 8.3–11.3 |
| TG lavas | 4–5.3 | 0.68–0.90 | 6.2–9.3 | 68–151 | 0.34–0.58 | 145–221 | 0.056–0.092 | 0.079–0.125 | 8.5–12 |
| MB lavas | 3.1–5 | 0.71–0.94 | 5.2–14.7 | 77–271 | 0.42–0.88 | 95–275 | 0.066–0.097 | 0.07–0.119 | 6.61–19.37 |

Data from Weaver (1991), Sun and McDonough (1989)

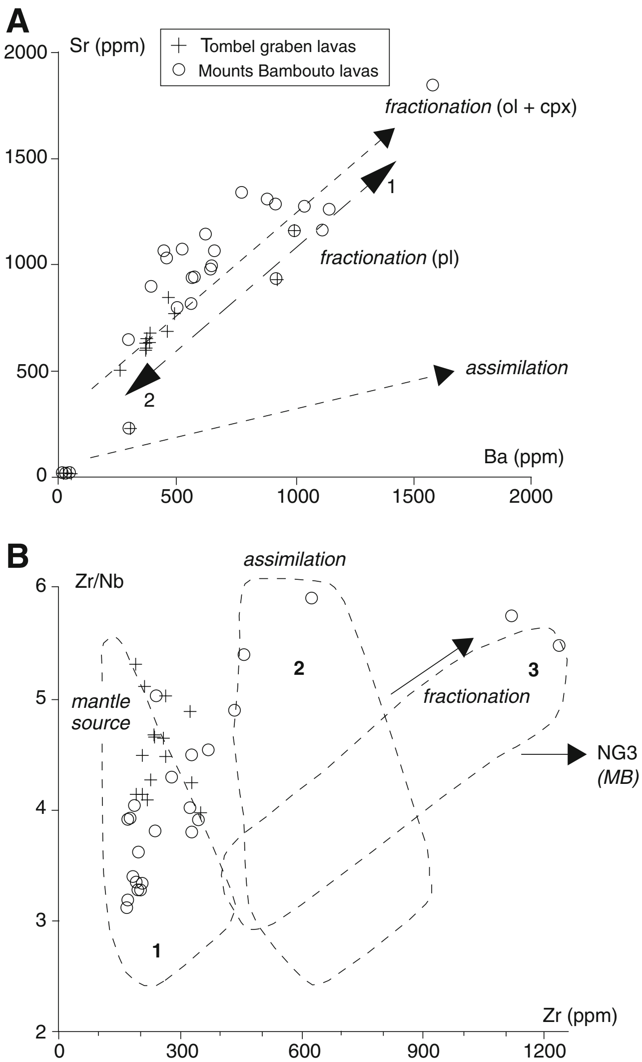


**Fig. 10 A** Sr vs. Ba diagram for Tombel graben and Mounts Bambouto lavas; fractionation and assimilation trends are shown (after Franz et al. 1999 modified). Fractionation of plagioclase has successively two effects (*arrow 1* then *arrow 2*, see text). **B** Zr/Nb vs. Zr diagram for Tombel graben and Mounts Bambouto lavas. *Dashed lines* show fields of rocks of Meidob Hills, Sudan (Franz et al. 1999) indicating a mantle source of mafic rocks (*1*) or assimilation for benmoreitic–trachytic pumices and lavas (*2*); the trend of fractionation is outlined (*3*)

deformation play a major role in creating pathways for magma ascent what has been established elsewhere in Africa. Farahat et al. (2006) mentioned that the Libyan low-volcanicity rift was probably related to the larger Afro-Arabian rift system. Chorowicz (2005) considered the East African Rift system, where many volcanoes have developed, as a unique succession of graben basins.

Judging from petrographical and geochemical data, one of the main differences between lavas of the two environments may be the size of the magma chamber. In Tombel graben, the magma could have formed in a small steady-state magma chamber, or it could be the consequence of some ephemeral magma bodies which produced either primitive xenoliths or Mg-rich basalts during an extensional period. In this case, undifferentiated mantle melts ascend directly to the surface. Thus, it seems that the recent activity (<2 Ma) of the Tombel graben area was characterized by an initial period of high eruptive rates with fissure eruptions of basalt. This was followed by a period of intermittent activity building numerous strombolian volcanoes. This activity is a consequence of the regional tectonic stress regime which was responsible for the faulting in this area. Tombel graben magma formed as a result of decompression that was induced by extensional faults. Differentiation is limited. The same phenomena probably created other collapse trenches or grabens (Mbo, Noun, Kumba, Tikar, a.s.o.) all along the CVL. Some of these troughs are more or less filled by volcanoes.

Minimum magma ascent velocity can be estimated as the presence of mantle xenoliths means that the ascent of the magma was quicker than the sinking down of the xenoliths. Sinking velocity of xenoliths is calculated from the Stokes' law: $v=(2/9).g.\Delta\rho.R^2/\eta_L$, where $g=9.81$, $\Delta\rho$ is the difference of density between the solid (3,300: olivine, opx, clinopyroxene and Fe–Ti oxides for Tombel; olivine for Bambouto) and the liquid (2,700 for hot basaltic liquid), that is to say 600, $R$ is 0.004 m, $\eta_L$ is about 100 Pa.s that is intermediate between 10 for very fluid basalt that gives pahoehoe lava and 1,000 for viscous block-lava. So we obtained a sinking velocity of $2\times10^{-4}$ m s$^{-1}$. It is established that the ascent velocity must be 10 to 100 times higher to carry xenoliths up to the surface, that is to say between $2\times10^{-3}$ and $2\times10^{-2}$ m s$^{-1}$. Such ascent velocities involve that crustal contamination could be only weakly effective during the magma ascent.

The large compositional range of Mounts Bambouto lavas, together with their petrographic characteristics (occurrence of xenocrysts, zoned crystals, coexistence of lavas of different chemical composition from basic to felsic) and morphological features (such as calderas, large lava flows, domes, necks) are in accord with the concept of a big, zoned, magma chamber in this area. Ascent of magma at the intersection of at least two directions of faults seems reasonable. Fractional crystallization occurs as mineral phases appear successively i.e. for basic lavas: Cr-spinel, then Fe–Ti oxides, olivine, clinopyroxene, plagioclase; for intermediate lavas: Fe–Ti oxides, then clinopyroxene, plagioclase, amphibole, alkali feldspar; for acid lavas: Fe–Ti oxides, then clinopyroxene and amphibole, plagioclase and alkali feldspar and some feldspathoids. Thick trachytic lava flows resulted from more extensive differentiation within the magma chamber accompanied by stoping and zone refining. Rejuvenation of tectonic movements associated with the upwelling of the asthenosphere has caused the periodic reactivation of the

**Table 4** Radiogenic isotope data (Sr, Nd) from Tombel graben and Mounts Bambouto selected samples (analyses *D Demaiffe*, Laboratoire de Géochimie Isotopique, Université Libre de Bruxelles, Belgique)

| Sample | Rock type | Rb (ppm) | Sr (ppm) | $^{87}Sr/^{86}Sr$ | 2σ | Sm (ppm) | Nd (ppm) | $^{143}Nd/^{144}Nd$ | 2σ | εNd |
|---|---|---|---|---|---|---|---|---|---|---|
| TTM1 (TG) | Basalt | 24.4 | 669 | 0.70342 | ±7 | 7.66 | 35.5 | 0.512873 | ±10 | 4.6 |
| TL1 (TG) | Hawaiite | 18.6 | 721 | 0.70345 | ±7 | 8.75 | 40.8 | 0.512918 | ±12 | 5.5 |
| TPL1 (TG) | Basalt | 16.7 | 847 | 0.703639 | ±7 | 9.92 | 47.1 | 0.512933 | ±9 | 5.8 |
| DB1 (MB) | Basanite | 27.3 | 968 | 0.703425 | ±5 | 7.57 | 37.7 | 0.512859 | ±8 | 4.3 |
| FR1 (MB) | Basanite | 34 | 1053 | 0.703248 | ±9 | 11.2 | 59.9 | 0.512863 | ±9 | 4.4 |
| EMI | | | | 0.7055 | | | | 0.51235 | | −5.6 |
| EMII | | | | 0.7075 | | | | 0.51265 | | 0.2 |
| HIMU M5 (Polynesia) | | | | 0.702791 | ±14 | | | 0.512892 | ±7 | 5.0 |
| HIMU M16 (Polynesia) | | | | 0.702821 | ±11 | | | 0.51290 | ±5 | 5.1 |
| FOZO | | | | 0.703–0.704 | | | | 0.5128–0.5130 | | 3.2–7.1 |

EMI and EMII from Faure (2001), HIMU=Magma source having a high ($^{238}U/^{204}Pb$) ratio (μ), HIMU compositions were taken from Woodhead (1996), EMI=Enriched mantle 1, EMII=Enriched mantle 2, CHUR (chondritic uniform reservoir)=0,512638 for $^{143}Nd/^{144}Nd$, FOZO=FOcal ZOne from Strake et al. (2005)

magma chamber, due to injections of new magma into the chamber. Contamination processes, always limited, seem to be more frequent in volcanoes on horsts like Mounts Bambouto than in volcanoes in grabens like Tombel graben: this is linked to the great amount of magma that was stored in the magma chamber below the horst volcano for a long time and thus had sufficient time to be contaminated.

Basanites of Tombel graben are primitive products of partial melting of the upper mantle with occasional contamination by other mantle domains as indicated by xenocrysts. Their young ages, their geochemical characteristic, as well as the presence in down-faulted troughs, reflect either the final activity of a main episode of activity in CVL or the beginning of a younger and new volcanic cycle.

Basanites of Mounts Bambouto contain only a small number of xenoliths but appear to be more primary according to their differentiation index (DI) (their lowest DI is 19.5 for BL4 rock from Mounts Bambouto against 22.2 for NT19 rock from Tombel graben).

Geochemically, basalts along the CVL differ in their degrees of melting of an otherwise nearly identically composed source material. Our studies suggest that both the pattern of tectonic stress and volcanic structure could explain the evolution of magmas along the CVL. As observed in Tombel graben and Mounts Bambouto volcanoes, lavas of the whole CVL had the same type of shallow asthenospheric mantle sources; compositional trends are similar to OIB basalts involving a dominant FOZO-type component and other components, like depleted MORB mantle (DMM) and variously enriched mantle (EMI and perhaps EMII). Hence, the distribution of Pliocene to Quaternary alkaline lavas along the CVL is fully consistent with the tectonic hot line model, related to asthenospheric upwelling. Our data are in agreement with one petrogenetic model for African basalts (King and Ritsema 2000; Pik et al. 2006). This model postulates that these basalts would result from a shallow mantle up-welling originating from depths within the asthenosphere and disseminated within the African plate across rejuvenated faults or uplifted swells.

**Acknowledgments** This work have been supported by the SCAC (Service de Coopération et d'Action Culturelle de la France au Cameroun), EGIDE (Centre français pour l'accueil et les échanges internationaux) and the French Government. D. Demaiffe carried out isotopic analyses at Laboratoire de Géochimie Isotopique, Université Libre de Bruxelles. J.C. Philippet has done K–Ar dating at Université de Bretagne Occidentale. L. Daumas has drawn the figures. B. Bonin, A.R. McBirney and B. Platevoet are thanked for useful remarks. Careful reviews by M. Okrusch, C. Breitkreuz and V. von Seckendorff have greatly improved the manuscript.

## References

Aït-Hamou F, Dautria JM, Cantagrel JM, Dostal J, Briqueu L (2000) Nouvelles données géochronologiques et isotopiques sur le volcanisme cénozoïque de l'Ahaggar (Sahara algérien): des arguments en faveur de l'existence d'un panache. C R Acad Sci Paris IIa 330(12):829–836

Allègre C (2005) Géologie isotopique. Belin, Paris

Bailey DK (1987) Mantle metasomatism—perspective and prospect. In: Fitton JG, Upton BGJ (eds) Alkaline igneous rocks. Geol Soc London Spec Publ 30:1–13

Ballentine CJ, Lee DC, Halliday AN (1997) Hafnium isotopic studies of the Cameroon line and new HIMU paradoxes. Chem Geol 139:111–124

Chorowicz J (2005) The East African rift system. J Afr Earth Sci 43:379–410

Deer WA, Howie RA, Zussman J (1966) An introduction to the rock-forming minerals. Longman, Essex, England

Déruelle B, Moreau C, Nkoumbou C, Kambou R, Lissom J, Njonfang E, Ghogomu RT, Nono A (1991) The Cameroon Line: a review. In: Kampunzu AB, Lubala RT (eds) Magmatism in extensional structural settings. Springer, Berlin, pp 274–327

Déruelle B, Ngounouno I, Demaiffe D (2007) The 'Cameroon Hot Line' (CHL): a unique example of active alkaline intraplate structure in both oceanic and continental lithospheres. C R Geoscience 339(9):589–600

Dumort JC (1968) Carte géologique de reconnaissance du Cameroun à l'échelle 1/500.000, feuille Douala-Ouest avec notice explicative. Imprimerie. Nationale, Yaoundé, Cameroun

Farahat ES, Abdel Ghani MS, Aboazom AS, Asran AMH (2006) Mineral chemistry of Al Haruj low-volcanicity rift basalts, Libya: Implications for petrogenetic and geotectonic evolution. J Afr Earth Sci 45–2:198–212

Faure G (2001) Origin of igneous rocks. The isotopic evidence. Springer, Berlin

Fitton JG (1983) Active versus passive rifting. Evidence from the West African rift system. Tectonophysics 94:473–481

Fitton JG (1987) The Cameroon line, West Africa: a comparison between oceanic and continental alkaline volcanism. In: Fitton JG, Upton BGJ (eds) Alkaline igneous rocks. Geol Soc London Spec Publ 30:273–291

Fitton JG, Dunlop HM (1985) The Cameroon Line, West Africa and its bearing on the origin of oceanic and continental alkali basalt. Earth Planet Sci Lett 72:23–38

Fosso J, Ménard JJ, Bardintzeff JM, Wandji P, Tchoua FM, Bellon H (2005) Les laves du mont Bangou: une première manifestation volcanique éocène, à affinité transitionnelle, de la Ligne du Cameroun. C R Geoscience 337:315–325

Franz G, Breitkreuz C, Coyle DA, El Hur B, Heinrich W, Paulick H, Pudlo D, Smith R, Steiner G (1997) The alkaline Meidob volcanic field (Late Cenozoic, northwest Sudan). J Afr Earth Sci 25–2:263–291

Franz G, Steiner G, Volker F, Pudlo D, Hammerschmidt K (1999) Plume related alkaline magmatism in central Africa—the Meidob Hills (W Sudan). Chem Geol 157:27–47

Gèze B (1943) Géographie physique et géologie du Cameroun occidental. Mémoire du Muséum National d'histoire Naturelle, Nlle série, t. XVII

Gourgaud A, Vincent PM (2004) Petrology of two continental alkaline intraplate series at Emi Koussi volcano, Tibesti, Chad. J Volc Geoth Res 129:261–290

Guille G, Goutière G, Sornein JF (1993) Les atolls de Mururoa et de Fangataufa (Polynésie française). I: Géologie–Pétrologie–Hydrogéologie, Edification et évolution des édifices. C.E.A., p 168

Halliday AN, Dickin AP, Fallick AE, Fitton JG (1988) Mantle dynamics: a Nd, Sr, Pb and O isotopic study of the Cameroon Line volcanic chain. J Petrol 29:181–211

Halliday AN, Davidson JP, Holden P, Dewolf C, Lee DC, Fitton JG (1990) Trace-element fractionation in plumes and the origin of HIMU mantle beneath the Cameroon Line. Nature 347 (6293):523–528

Hart SR (1988) Heterogeneous mantle domains: signatures, genesis and mixing chronologies. Earth Planet Sci Lett 90:273–296

Kagou Dongmo A (2006) Le mont Manengouba: Evolution volcanologique, caractères magmatologiques et risques naturels; comparaison avec les monts Bambouto et Bamenda (Ligne du Cameroun). Thèse Doct d'Etat, Univ Yaoundé I, Cameroon

Kagou Dongmo A, Wandji P, Pouclet A, Vicat JP, Cheilletz A, Nkouathio DG, Alexandrov P, Tchoua FM (2001) Evolution volcanologique du mont Manengouba (Ligne du Cameroun), nouvelles données pétrographiques, géochimiques et géochronologiques. C R Acad Sci, IIA, 333:155–162

Kil YW (2007) Geochemistry and petrogenesis of spinel lherzolite xenoliths from Boeun, Korea. J Asian Earth Sci 29:29–40

King SD, Ritsema J (2000) African hot spot volcanism: small-scale convection in the upper mantle beneath cratons. Science 290:1137–1140

Kuepouo G, Tchouankoue JP, Nagao T, Sato H (2006) Transitional tholeiitic basalts in the Tertiary Bana volcano–plutonic complex, Cameroon Line. J Afr Earth Sci 45:318–332

Kueté M, Dikoumé A (2000) Espace, pouvoir et conflits dans les Hautes Terres de l'Ouest Cameroun. Collect. Sociétés. Presses Universitaires de Yaoundé, p 149

Le Maitre RW (ed) (2002) Igneous rocks. A classification and glossary of terms. Recommendations of the International Union of Geological Sciences Subcommission on the Systematics of Igneous Rocks. Cambridge University Press, Cambridge, UK

Lee DC, Halliday AN, Fitton JG, Poli G (1994) Isotopic variations with distance and time in the volcanic islands of the Cameroon Line—evidence for a mantle plume origin. Earth Planet Sci Lett 123:119–138

Maluski H, Coulon C, Popoff M, Baudin P (1995) $Ar^{40}/Ar^{39}$ chronology, petrology and geodynamic setting of Mesozoic to Early Cenozoic magmatism from the Benue Trough, Nigeria. J Geol Soc London 152:311–326

Marzoli A, Renne PR, Piccirillo EM, Francesca C, Bellieni G, Mel AJ, Nyobe JB, N'ni J (1999) Silicic magmas from the continental Cameroon Volcanic Line (Oku, Bambouto and Ngaoundéré): $^{40}Ar/^{39}Ar$ dates, petrology, Sr-Nd-O isotopes and their petrogenetic significance. Contrib Mineral Petrol 135:133–150

Marzoli A, Piccirillo EM, Renne PR, Bellieni G, Iacumin M, Nyobe JB, Tongwa AT (2000) The Cameroon Volcanic Line revisited: Petrogenesis of continental basaltic magmas from lithospheric and asthenospheric mantle sources. J Petrol 41:87–109

Meyers JB, Rosendahl BR, Harrison CGA, Ding ZD (1998) Deep-imaging seismic and gravity results from the offshore Cameroon Volcanic Line, and speculation of African hotlines. Tectonophysics 284:31–63

Montigny R, Ngounouno I, Déruelle B (2004) Ages K-Ar des roches magmatiques du fossé de Garoua (Cameroon): leur place dans le cadre de la Ligne du Cameroun. C R Geoscience 336:1463–1471

Morimoto N, Fabriès J, Fergusson A, Ginzburg I, Roos M, Seifert F, Zussman J (1988) Nomenclure of pyroxenes. Bull Mineral 111:535–550

Moundi A (2004) Les basaltes des plateaux du plateau Bamoun: pétrologie-géochimie et géochronologie, implications sur les sources des magmas, leur contexte et évolution géodynamique. Thèse Doct d'Etat, Univ Yaoundé I, Cameroon

Moundi A, Wandji P, Bardintzeff JM, Ménard JJ, Okomo Atouba LC, Mouncherou OF, Reusser E, Bellon H, Tchoua FM (2007) Les basaltes éocènes à affinité transitionnelle du plateau Bamoun, témoins d'un réservoir mantellique enrichi sous la Ligne Volcanique du Cameroun. C R Geoscience 339:396–406

Nekvasil H (1994) Ternary feldspar/melt equilibria: a review. In: Parsons I (ed) Feldspars and their reactions. NATO ASI Series, Series C: Mathematical and Physical Sciences, 421. Kluwer, Dordrecht, pp 195–219

Ngako V, Njonfang E, Tongwa Aka F, Affaton P, Metuk Nnange J (2006) The North–South Paleozoic to Quaternary trend of alkaline magmatism from Niger–Nigeria to Cameroon: Complex interaction between hotspots and Precambrian faults. J Afr Earth Sci 45–3:241–256

Ngounouno I, Déruelle B, Guiraud R, Vicat JP (2001) Magmatismes tholéiitique et alcalin des demi-grabens crétacés de Mayo Oulo–Léré et de Babouri–Figuil (Nord du Cameroun–Sud du Tchad) en domaine d'extension continentale. C R Acad Sci 333:201–207

Nimis P, Ulmer P (1998) Clinoyroxene geobarometry of magmatic rocks. Part 1: An expanded structural geobarometry for anhydrous and hydrous, basic and ultrabasic systems. Contrib Mineral Petrol 133:122–135 (Erratum, pp 314–327)

Njonfang E, Nono A (2003) Clinopyroxene from some felsic alkaline rocks of the Cameroon Line, Central Africa: petrological implications. Eur J Mineral 15:527–542

Nkouathio DG (2006) Evolution tectono-magmatique et volcanologique de la Ligne du Cameroun: comparaison d'un volcanisme de graben (plaine de Tombel) et d'un volcanisme de horst (monts Bambouto). Thèse Doct d'Etat, Univ Yaoundé I, Cameroon

Nkouathio DG, Ménard JJ, Wandji P, Bardintzeff JM (2002) The Tombel graben (West Cameroon): a recent monogenetic volcanic field of the Cameroon Line. J Afr Earth Sci 35:285–300

Nkouathio DG, Kagou Dongmo A, Wandji P, Bardintzeff JM, Tchoua FM (2006) Evolution and tectonic control of volcanism along the Cameroon Volcanic Line: case study of graben and horst volcanoes. Implication on the nature of volcanic hazards. Garavolcan, 300th Int Conf commemorating the 1706 Arenas Negras Eruption, Garachico, Tenerife, Canary Islands, May 22–27, 2006

Nono A, Njonfang E, Kagou Dongmo A, Nkouathio DG, Tchoua FM (2004) Pyroclastic deposits of the Bambouto volcano (Cameroon Line, Central Africa): evidence of a strombolian initial phase. J Afr Earth Sci 39:409–414

Peccerillo A, Barberio MR, Yirgu G, Ayalew D, Barbieri M, Wu TW (2003) Relations between mafic and peralkaline silicic magmatism in continental rift settings: a petrological, geochemical and isotopic study of the Gedemsa Volcano, Central Ethiopian Rift. J Petrol 11:2003–2032

Peccerillo A, Donati C, Santo AP, Orlando A, Yirgu G, Ayalew D (2007) Petrogenesis of silicic peralkaline rocks in the Ethiopian rift: Geochemical evidence and volcanological implications. J Afr Earth Sci 48:161–173

Pik R, Marly B, Hilton DR (2006) How many plumes in Africa ? The geochemical point of view. Chem Geol 226:100–114

Rollinson H (1993) Using geochemical data: evaluation, presentation, interpretation. Longman, Harlow, Essex, UK

Sato H, Aramaki S, Kusakabe M, Hirabayashi JI, Sano Y, Nojiri Y, Tchoua FM (1990) Geochemical difference of basalts between polygenetic and monogenetic volcanoes in the Central part of the Cameroon volcanic line. Geochem J 24:357–370

Steiger RH, Jäger E (1977) Subcommission on geochronology: convention on the use of decay constants in geo- and cosmochronology. Earth Planet Sci Lett 36:359–362

Stracke A, Hofman AW, Hart SR (2005) FOZO, HIMU, and the rest of the mantle zoo. Geochem Geophys Geosyst 6(5):Q05007 doi:10.1029/2004GC000824

Sun SS, McDonough WF (1989) Chemical and isotopic systematics of oceanic basalts: implications for mantle composition and processes. In: Saunders AD and Norry MJ (eds) Magmatism in the oceans basins. Geol Soc London Spec Publ 42:313–345

Tchoua FM (1974) Contribution à l'étude géologique et pétrologique de quelques volcans de la «Ligne du Cameroun» (Monts Manengouba et Bambouto). Thèse Doct d'Etat, Univ Clermont-Ferrand, France

von Wolff F (1914) Der Vulkanismus. Band I. Allgemeiner Teil. Enke, Stuttgart

Walker GPL (2000) Basaltic volcanoes and volcanic systems. In: Sigurdsson H, Houghton BF, McNutt SR, Rymer H, Stix J (eds) Encyclopedia of volcanoes. Academic Press, New York, pp 283–289

Weaver BL (1991) Trace element evidence for the origin of ocean island basalts. Geology 19:123–126

Wilson M, Downes H (1991) Tertiary-Quaternary extension-related alkaline magmatism in Western and Central Europe. J Petrol 32 (4):811–849

Wilson M, Guiraud R (1992) Magmatism and rifting in western and Central Africa from late Jurassic to recent times. Tectonophysics 123:203–225

Woodhead JD (1996) Extreme HIMU in an oceanic setting: the geochemistry of Mangaia Island (Polynesia), and temporal evolution of the Cook-austral hotspot. J Volc Geoth Res 72:1–19

Youmen D (1994) Evolution volcanologique, pétrologique et temporelle de la caldera des monts Bambouto (Cameroun). PhD Thesis. Universität Kiel, Germany

Zindler A, Hart S (1986) Chemical geodynamics. Ann Rev Earth Planet Sci Lett 14:493–571